Terms, definitions and measurements to describe sonographic features of myometrium and uterine masses: a consensus opinion from the Morphological Uterus Sonographic Assessment (MUSA) group

van den Bosch, T.; Dueholm, M.; Leone, F. P. G.; Valentin, Lil; Rasmussen, C. K.; Votino, A.; van Schoubroeck, D.; Landolfo, C.; Installe, A. J. F.; Guerriero, S.; Exacoustos, C.; Gordts, S.; Benacerraf, B.; D'Hooghe, T.; de Moor, B.; Brolmann, H.; Goldstein, S.; Epstein, E.; Bourne, T.; Timmerman, D.

Published in:
Ultrasound in Obstetrics & Gynecology

DOI:
10.1002/uog.14806

2015

Document Version:
Peer reviewed version (aka post-print)

TERMS AND DEFINITIONS FOR DESCRIBING MYOMETRIAL PATHOLOGY USING ULTRASONOGRAPHY

[1]Thierry Van den Bosch, [2]Margit Dueholm (joint first author), [3]Francesco Paolo Giuseppe Leone, [4]Lil Valentin, [2]Christina Kjaergaard Rasmussen, [5]Angelo Votino, [1]Dominique Van Schoubroeck, [6]Chiara Landolfo, [7,8]Arnaud JF Installé, [9]Stefano Guerriero, [10]Caterina Exacoustos, [11]Stephan Gordts, [12]Beryl Benacerraf, [13]Thomas D'Hooghe, [7,8]Bart De Moor, [14]Hans Brölmann, [15]Steven Goldstein, [16]Elisabeth Epstein, [17,1]Tom Bourne, [1]Dirk Timmerman

[1]Department of Obstetrics and Gynecology, University Hospitals KULeuven, Belgium, [2]Department of Obstetrics and Gynecology, Aarhus University Hospital, Aarhus, Denmark, [3]Department of Obstetrics and Gynecology, Clinical Sciences Institute L Sacco, University of Milan, Milan, Italy, [4]Department of Obstetrics and Gynecology, Skåne University Hospital, Lund University, Malmö, Sweden, [5]Department of Obstetrics and Gynecology, Brugmann University Hospital, Brussels, Belgium, [6]Department of Obstetrics and Gynecology, Sant'Orsola-Malpighi Hospital, University of Bologna, Bologna, Italy, [7]KU Leuven, Department of Electrical Engineering (ESAT), STADIUS, Center for Dynamical Systems, Signal Processing and Data Analytics, Leuven, Belgium, [8]iMinds Medical IT, Leuven, Belgium, [9]Department of Obstetrics and Gynaecology, Azienda Ospedaliera Universitaria of Cagliari and University of Cagliari, Cagliari, Italy, [10]Department of Biomedicine and Prevention, Obstetrics and Gynecological Clinic, University of Rome "Tor Vergata", Italy, [11]L.I.F.E. *(*Leuven Institute for Fertility & Embryology), Leuven, Belgium, [12]Departments of Radiology and Obstetrics & Gynecology, Harvard Medical School, USA, [13]Leuven University Fertility Centre, University Hospitals KULeuven, Belgium, [14]Department of Obstetrics and Gynecology, VU University Medical Center, Amsterdam, the Netherlands, [15]Department of Obstetrics and Gynecology, New York University School of Medicine, New York, USA, 16Department of Obstetrics and Gynecology, Karolinska University Hospital, Stockholm, Sweden, [17]Queen Charlotte's and Chelsea Hospital, Imperial College, London, UK

SHORT TITLE: MUSA consensus

KEY WORDS: uterus, myometrium, adenomyosis, fibroids, leiomyosarcoma, ultrasonography, consensus

CORRESPONDENCE: Thierry Van den Bosch, MD, PhD, Department of Obstetrics and Gynecology, University Hospitals KULeuven, Herestraat 49, 3000 Leuven, Belgium, thierryvandenbosch1901@gmail.com

Tel +32-16-343642

ABSTRACT:

This paper is a consensus statement on terms, definitions and measurements to describe and report the sonographic features of the myometrium using grayscale sonography, color/power Doppler, and three-dimensional ultrasound imaging.

These terms and definitions may be relevant both for the clinician when reporting ultrasound examinations in daily practice and for clinical research. The use of the terminology when describing the two most common myometrial lesions (fibroids and adenomyosis) is presented.

Abbreviations:

Ultrasonography (US),

Transvaginal ultrasonography (TVS),

Two-dimensional (2D),

Three-dimensional (3D),

Volume Contrast Imaging (VCI),

Endomyometrial junctional zone (JZ),

Total myometrial wall thickness (TWT)

Maximum thickness of the junctional zone (JZ_{max})

Minimum thickness of the junctional zone (JZ_{min})

Difference between maximal and minimal JZ thickness (JZ_{dif})

Penetration (P)

INTRODUCTION

A variety of disorders or pathology in the uterus gives rise to different manifestations and clinical signs. Ultrasonography (US) is a first-stage imaging technique for assessing the myometrium and requires findings to be reported consistently. Recently the FIGO PALM-COEIN system (polyp; adenomyosis; leiomyoma; malignancy and hyperplasia; coagulopathy; ovulatory dysfunction; endometrial; iatrogenic; not yet classified)[1;2] has been published, classifying the etiology of abnormal uterine bleeding, including the myometrial pathologies adenomyosis and fibroids. However, the implementation of this classification in daily clinical practice is hampered by the lack of standardization of terms and definitions used to describe ultrasound findings. Standardized terms to be used when describing ultrasound images of the endometrium and uterine cavity have been suggested by the IETA group[3]. However, there is still no standardized terminology for describing ultrasound images of normal and pathological myometrium as well as uterine masses[4].

In clinical practice and research, standardized reporting of ultrasound findings with regard to the myometrium is essential to reduce intra- and inter-observer variability in the evaluation of pathology, to assess the effect of medical or surgical treatment, and to compare ultrasound imaging with other imaging techniques. Moreover, a common terminology is necessary for comparison between studies and when combining data in meta-analyses. Reliable predictors of benign pathology is essential clinically to allow safe use of minimally invasive techniques for the treatment of uterine myomas such as selective uterine artery embolization, fibroid ablation or laparoscopic morcellation[5].

The primary aim of this paper is to present a consensus opinion on the terminology to be used when describing the ultrasonographic features of the myometrium and of myometrial lesions. These terms and definitions should be relevant both for clinicians reporting ultrasound examinations in day to day practice and for clinical research. The secondary aim is to illustrate the use of the terminology when describing the two most common myometrial lesions: fibroids and adenomyosis.

METHODOLOGY

This consensus paper is based on the opinion of a panel of clinicians (MUSA, Morphological Uterus Sonographic Assessment) with expertise that includes gynecological ultrasonography, fertility treatment, hysteroscopy, general gynecology and clinical research. Amongst the authors are members from the IOTA (International Ovarian Tumor Analysis) and IETA (International Endometrial Tumor Analysis) groups and in order to produce a consensus paper that includes opinions from both ultrasound and endoscopic interest groups, members of the ESGE (European Society of Gynaecological Endoscopy) are also included. A first draft was written in April 2014 by the two first authors and sent to all co-authors. All co-authors had the opportunity to comment within a fixed time limit. Reply was mandatory for co-authorship. After taking all comments into account a revised draft was sent to all co-authors. In the event of conflicting opinions a consensus was proposed after discussion between the two first authors and the last author. This pathway was repeated until a consensus between all authors was reached. After seven revisions the manuscript was deemed ready for submission.

SCANNING THE MYOMETRIUM (DETAILED DESCRIPTION)

Ultrasound examination of the myometrium may be performed using transabdominal or transvaginal scanning. Although transvaginal ultrasonography (TVS) is generally preferred, transabdominal ultrasonography may be necessary for imaging beyond the small pelvis. For adequate visualization of the uterus, some bladder filling is required to displace the small bowel from the field of view. Image quality during transabdominal ultrasonography may also be hampered by adipositas, scar tissue or uterine retroversion.

High-resolution TVS allows for detailed assessment of the myometrium within a limited depth of view. Transabdominal ultrasonography may be necessary for imaging beyond the small pelvis. A TVS starts with a dynamic two-dimensional (2D) scan of the uterus in two perpendicular planes. Some gentle pressure may need to be applied with the probe or the free hand to assess uterine mobility and to screen for site specific tenderness[6].

On a sonographic cross-section through the uterus, the arcuate venous and arterial vessels can be seen close to the outer myometrial border. The junctional zone (JZ) (also referred to as inner myometrium, archimyometrium or

stratum subvasculare) is visible as a hypoechogenic subendometrial halo. This layer is composed of longitudinal and circular closely packed smooth muscle fibers[7].

Three dimensional (3D) ultrasonography makes off-line examination and manipulation of ultrasound images possible. This may facilitate accessing a second opinion by an expert examiner in difficult cases**.** 3D volume acquisition of the uterus starts with an adequately enlarged mid-sagittal or transverse section of the uterine body. In optimal conditions the mid-sagittal plane allows the visualization of the entire length of the endometrium as well as the endocervical canal. The acquisition angle is chosen to include the entire uterine volume of interest. Once the 3D volume has been acquired, examination of the volume is performed in the multiplanar view by scrolling in each sectional plane separately.

Coronal sections provide information on the external contour of the uterus and cavity shape.
Different features for image optimization and post-processing are used. For example, rendering and Volume Contrast Imaging (VCI) modes deliver details on the continuity and thickness of the junctional zone (JZ)[8-10]. Other post processing modalities such as the use of tomographic ultrasound imaging (also called multi-slice imaging) may also be helpful.

UTERINE MEASUREMENTS, SHAPE AND **EXTERNAL CONTOUR**.

Measuring the corpus of the uterus is performed as shown in Figure 1. If the aim of the ultrasound scan is to evaluate the myometrium (e.g. in the diagnosis of adenomysosis), then measurement of the uterine volume should exclude the cervix. If the length of the entire uterus (including the cervix) is required (e.g. at preoperative evaluation), the sum of the corpus length and the cervical length should be reported.
The corpus length (d1) is the sum of the fundus length (from the fundal serosal surface of the uterus to the fundal tip of the endometrial cavity) and the endometrial cavity length (from the fundal tip of the endometrial cavity to the internal os of the cervix). Both should preferentially be measured separately in the longitudinal plane of the uterus. The largest antero-posterior diameter (d2) is also measured in the sagittal plane. The largest transverse diameter is measured in the transverse plane of the uterus. The formula for the volume calculation based on these

measurements is displayed in Table 1 and in Figure 1. If the length of the entire uterus is required, the sum of the total length of the uterus (d1) and the cervical length should be reported.

The **serosal contour** of the uterus is reported as *regular or lobulated* (Figure 2).

The **anterior and posterior myometrial walls** are measured from the external uterine serosa to the external endometrial contour and should include the JZ, but not the endometrium. The myometrial walls are measured in the sagittal plane perpendicular to the endometrium. Both measurements are taken on the same image, and the measurements are taken where the myometrial wall appears to be at its thickest. The ratio between the anterior and posterior wall thickness is calculated. A ratio between the anterior and posterior wall thickness of around 1 means that the myometrial walls are symmetrical. A ratio well above or below 1 indicates asymmetry, although this may also be estimated subjectively (Figure 3). The myometrial walls can also be measured in the transverse or coronal planes if felt to be necessary.

THE JUNCTIONAL ZONE

Although the JZ can often be visualized on 2D ultrasound, acquisition of a 3D-volume enables a more complete assessment in the sagittal, transverse and coronal plane as shown in a standardized multi-planar view[11] (Figure 4). Using the standardized multi-planar view reduces inter-observer variation in measurements, is used in general clinical practice for evaluation of the coronal view[12], and may be obtained by the z-rotation technique[13]. Imaging the JZ may be optimized by using a post-processing rendering mode, for example Volume Contrast Imaging (VCI). The thickness of the slices or render box may be selected between 1 and 4 mm[9].

The JZ (Table2 and Figure 5) may be regular, irregular, interrupted, not visible, not assessable[3] or may manifest more than one feature (e.g. irregular and interrupted). For research purposes, any irregularity in the JZ may be described (e.g. cystic areas, hyperechogenic dots, hyperechogenic buds and lines) in each location (anterior, posterior, lateral left, lateral right, fundus) according to the specific research protocol.

Detailed morphological assessment and measurement of the JZ is generally only currently relevant in the context of research protocols. The JZ and the total myometrial wall thickness (TWT) are measured perpendicular to the

endometrium on the same section through the uterus. The maximum *thickness* of the junctional zone (JZ_{max}) is measured at the area where the JZ appears to be at its thickest, and the minimum thickness JZ_{min} where it appears to be at its thinnest, after evaluation of the total three-dimensional volume of the uterus (Figure 6). To define the *ratio* between the JZ and the total uterine wall thickness, both the JZ and the total uterine wall thickness should be measured on the same image. Where to take the measurement(s) to calculate this ratio depends on the research protocol. If the JZ is ill-defined or not visible, it should be reported as 'non-measurable'.

The *magnitude* and the *extent* of any irregularity of the JZ may be reported and the *location* of the JZ irregularity (anterior, posterior, lateral left, lateral right, fundus) specified according to the research protocol. The *magnitude* of a JZ irregularity is expressed as the difference between the maximal and minimal JZ thickness: (JZ_{max}) - (JZ_{min}) = JZ_{dif}. The *extent* of JZ irregularity is reported as the subjective estimation of the percentage of the JZ that is irregular (<50% or $\geq$50%). This estimation can be made for the uterus as a whole or for each location. *Interruption* of the JZ may be caused by focal infiltration of the JZ by endometrial tissue, but contractions and changes within the JZ may also give rise to apparent JZ irregularities or influence JZ thickness. The extent of interruptions are recorded as a subjective estimation of the percentage of the JZ that is interrupted (<50% or $\geq$50%). Again this may be for the uterus as a whole or in each specific location.

DESCRIPTION OF MYOMETRIAL PATHOLOGY (Table 1)

The overall **echogenicity** of the myometrium is reported as *homogeneous* or *heterogeneous*. The reason for the heterogeneity (e.g. cysts, shadowing) should be specified as outlined below.

Myometrial pathology may be *localized* (one or more 'lesions') or *diffuse.* A myometrial lesion may be *well-defined* as typically seen in fibroids or *ill-defined* as typically seen in adenomyosis. Each lesion should be described according to its *location, size,* and *site* (Table 1 and Figures 7-9). The site and size may be impossible to describe for some ill-defined lesions.

The lesion **location** within the myometrium may be anterior or posterior, fundal, right lateral or left lateral. A lesion is *global* if the pathology diffusely involves the whole myometrium.

The **site** of a well-defined lesion should be reported using the **FIGO classification** for fibroids: 0 = pedunculated intracavitary; 1 = submucosal <50% intramural; 2 = submucosal ≥50% intramural; 3 = 100% intramural, but contacts the endometrium; 4 = intramural; 5 = subserosal ≥50% intramural; 6 = subserosal <50% intramural; 7 = subserosal pedunculated; 8 = other (e.g. cervical, parasitic)[1;14](Figure 7). Lesion ***size*** is estimated by measuring the three largest orthogonal diameters.

The minimal distance from the lesion to the endometrium (*inner lesion free margin, IFM*) and serosal surface (*outer lesion free margin, OFM*) of the uterus[15;16] is measured as described in Figure 8.

Ill-defined lesions are by definition difficult to delineate and measurements may be inaccurate. The *extent* of an ill-defined lesion can be estimated subjectively as the percentage of the myometrium of the whole uterine volume that is involved. If less than 50% of the total myometrium is involved, the lesion is reported as *localized,* if at least 50% of the myometrium is involved, it is reported as *diffuse*. For research purposes or in a preoperative setting, the percentage involved in each location may need to be recorded. For ill-defined lesions, the *penetration (P)* is defined as the ratio between the maximal thickness of the lesion and the total uterine wall thickness. The penetration is measured where the lesion appears to be at its largest as shown in Figure 9.

The **echogenicity** of a lesion is reported as *uniform* (homogeneous and/or symmetrical pattern of echogenicity) or *non-uniform* (heterogeneous) (Figure 10a). A uniform lesion may be *hypo-, iso- or hyperechogenic*.

For research purposes, the echogenicity of the lesion may be compared to the adjacent myometrium and semi-quantified as shown in Figure 10b (very hypoechogenic--, hypoechogenic-, isoechogenic, hyperechogenic+ or very hyperechogenic++).

A lesion may have non-uniform echogenicity because of mixed echogenicity, the presence of echogenic areas or of cystic areas (regular or irregular). If present, cyst contents may be anechoic, of low-level echogenicity, of ground glass appearance or of mixed echogenicity[17]. Anechoic areas can be differentiated from large vessels by using power Doppler to confirm the absence of blood flow.

The **rim** of a lesion may be ill-defined, hypo-, or hyper-echogenic in comparison to the myometrium (Figure 11), and the **shape** of a lesion may be *round* or *not-round*. A lesion that is *not-round* may be *oval, lobulated* or *irregular* (Figure 11).

Shadowing (Figure 12a) may arise from the edge of a lesion in which case they are reported as **edge shadows**, or from areas within the lesion when they are termed **internal shadows**. The degree of shadowing is reported subjectively as slight, moderate or strong.

Fan-shaped shadowing (Figure 12b)**.** Fan-shaped *shadowing* is defined as the presence of hypoechogenic linear stripes, sometimes alternating with linear hyperechogenic stripes. Fan-shaped shadowing may be caused by overlying (micro)cystic structure(s). The degree of shadowing is subjectively recorded as slight, moderate or strong.

Cysts (Figure 13a). Myometrial *cysts* are rounded lesions within the myometrium. The cyst contents may be anechoic, of low-level echogenicity, ground glass appearance or mixed echogenicity. A cyst may be surrounded by a *hyperechogenic rim*. In the context of research studies, the number of cysts and the largest diameter of the largest cyst or of a specified number of cysts, as well as the echogenicity of the cyst fluid may be reported. Some cysts are not measurable individually and may form aggregates of tiny, hypoechogenic microcysts (anechoic lacunae) within the myometrium. There are often several aggregates of microcysts in an area.

Hyperechogenic islands (Figure 13b). These are hyperechogenic areas within the myometrium and they may be regular, irregular or ill-defined. The number and the maximum diameter of the largest hyperechogenic island (or, if applicable, for example as part of a research protocol, of a specified number of hyperechogenic islands) may be reported. Hyperechogenic islands should be distinguished from small hyperechogenic spots seen in the subendometrium (Figure 13c).

Hyperechogenic subendometrial lines or buds (Figure 14). The JZ may be disrupted by *hyperechogenic subendometrial lines or buds***.** Hyperechogenic subendometrial lines are (almost) perpendicular to the endometrial cavity and are in continuum with the endometrium. These buds and lines should be distinguished from small hyperechogenic spots seen in the subendometrium (Figure 13c). For research purposes, the number and location of the subendometrial lines or buds may be reported.

Vascularization of the myometrium and myometrial lesions

When using **color or power Doppler** the arcuate vessels of the uterus are often visible at the periphery of the myometrium running parallel to the uterine serosa. Perpendicular to the arcuate vessels, the radial arteries and veins flowing throughout the myometrium are usually detectable (Figure 15).

Power Doppler is preferred to color Doppler because in general it is superior for the detection of small vessels with low blood flow velocities. Color Doppler is used to assess the direction of blood flow. Depending on the area of interest, the color or power Doppler box should include the whole or a specific part of the uterus, or be focused on a myometrial lesion. Magnification and settings should be adjusted to ensure maximum sensitivity, and the Doppler gain should be reduced until all colour artefacts disappear. Usually settings allowing the detection of blood flow velocities of 3-9 cm/sec are optimal, but this may vary from one ultrasound machine to another.

The vascular pattern within the myometrium may be *uniform* or *non-uniform* (Figure 16).

The vascular pattern of a myometrial lesion may be *circumferential, intra-lesional* or *both* circumferential and intra-lesional (Figure 16).

Some lesions are associated with disruption of the normal uterine vasculature, while others are not. *Trans-lesional vascularity* (Figure17) is characterized by the presence of vessels, perpendicular to the uterine cavity/serosa crossing the lesion.

The degree of vascularization should be reported using a subjective *color score* (color score 1 representing no color and color score 4 abundant color signals). The color score is based on the subjective evaluation of both the percentage of the lesion being vascularized and the color hue. The color score is assigned taking into account the lesion as a whole, but in lesions with uneven internal vascularization (e.g. because of cystic areas or central necrosis) the score reflects the degree of vascularization in the solid parts of the lesion. If there is an uneven spread of vascularization in the solid components of the lesion, the score for the most vascularized solid component and the

percentage of the solid components with color signals may be recorded. A color score may be assigned separately to circumferential and intra-lesional vascularity (Figure 18).

When carrying out research studies, the vascularity of lesions may be reported as iso-, hypo- or hyper-vascular compared to the vascularity of the surrounding myometrium. Reporting a lesion's vascularity may include the *number* of vessels (single or multiple), vessel *size* (small and equal, large and equal, unequal; or the vessel diameter may be measured), the *direction* of vessels (perpendicular or not perpendicular to endometrium), the vessel *branching pattern* (no branching, regular branching, irregular branching) and may be further specified as outlined in Table 3 and in Figure 19. Irregular branching vessels may be defined as abnormal tortuous vessels, irregular caliber vessels, a lack of hierarchy in branching with varying branching angles, vessels sprouts and an overall impression of a chaotic vessel pattern. The term c*ircumferential* vessels relates to vessels that surround a lesion, whereas vessels located inside a lesion are called *intra-lesional*.

Again within the context of research, color flow within a lesion may be quantified using 3D ultrasound with virtual organ computer-aided analysis (VOCAL) in order to calculate 3D power Doppler indices: the *vascularity index* (VI: number of color voxels in the volume expressed as a percentage of the total number of voxels in the volume), the *flow index* (FI: mean color value in the color voxels expressed as a number from 0-100) and the *vascularization-flow index* (VI multiplied with FI: VFI reflects the mean color value in all the volume's voxels expressed as a number from 0-100) potentially reflecting vascularity, flow velocity and tissue perfusion, respectively [18;19]. However, because 3D vascular indices depend on machine settings, there remains doubt about their reproducibility and their clinical use has yet to be adequately explored [19]. Until the pitfalls with these indices have been resolved, we recommend not using them outside the context of a specific research project.

SCANNING THE MYOMETRIUM IN GENERAL CLINICAL PRACTICE

In general clinical practice reporting on the myometrium may be more succinct, as summarized in Table 4.

The uterine corpus is measured, the symmetry of the myometrial walls is estimated and the overall echogenicity of the myometrium is reported as homogenous or heterogeneous.

In the presence of a myometrial lesion, it is specified if the lesion is well defined or ill defined. The number (or the estimated number if > 4 lesions) of lesions is reported as well as the location, the site and maximal diameter of the clinically relevant lesion(s).

The presence of shadowing, myometrial cysts, hyperechogenic islands or subendometrial echogenic lines and buds is reported.

The junctional zone is reported as 'regular' or 'poorly defined' (if irregular, interrupted, not visible or not assessable).

When it is clinically relevant to evaluate vascularity, the overall vessel pattern within the myometrium of the whole uterus is reported as uniform or non-uniform. The amount of color within a lesion is reported using the color score (1 = no color; 2 = minimal color; 3 = moderate color; 4 = abundant color).

We propose to include the following ultrasound pictures when reporting on the myometrium (ultrasound images of the endometrium should be described using the IETA terminology[3]):

- at least one mid-sagittal section of the uterus (gray scale and with power Doppler)
- preferably also a transverse section and/or a coronal 3D-reconstruction of the uterus
- if a lesion is seen, at least one section of the uterus including the lesion
- preferably also a detailed (zoomed) image of the lesion (in gray scale and with power Doppler)
- for the mapping of fibroids 3D-imaging showing the three standard orthogonal planes through the uterus or tomographic ultrasound images (TUI) may sometimes be illustrative.

ULTRASOUND FINDINGS ASSOCIATED WITH PATHOLOGY

In this section we describe ultrasound features that in the opinion of the authors and on the basis of reports in the literature, are thought to be associated with pathology and in particular with fibroids and adenomyosis (see summary in table 5). Further research should validate the importance of each of these features.

ADENOMYOSIS

Adenomyosis is caused by a proliferation of endometrial glands and stroma leading to ill-defined lesions within the myometrium. Adenomyosis may be present on one or more sites within the uterine wall or involve most of the myometrium and may often be dispersed within the myometrium rather than forming a confined lesion: i.e. *diffuse adenomyosis*. On the other hand if adenomyosis is present in only one part of the myometrium, it is called *focal adenomyosis*. In rare cases it may present as a large cyst (an *adenomyotic cyst* or *cystic adenomyoma*)[20-24]. On histological examination, adenomyosis is classified as *diffuse* when endometrial glands or stroma are distributed diffusely in the myometrium, and *focal* when circumscribed nodular aggregates are seen. Focal adenomyosis is not the same as an adenomyoma. These are defined by pathologists as focal adenomyosis with additional compensatory hypertrophy of the surrounding myometrium[25].

The ultrasound features of adenomyosis (Figure 20) should be reported and quantified (Table 1-3). The ultrasound features of a globular uterus with ill- defined adenomyotic lesions may be explained by direct invasion of endometrial tissue from the endometrium as seen in “classic adenomyosis”, or invasion from endometriotic implants on the serosal surface of the uterus[26]. More seldom diffuse adenomyosis may be localized as a solitary finding without direct continuation with the serosa or the endometrium[22]. The proportion of endometrial glandular structures, endometrial stroma and hypertrophic muscle elements within a lesion probably explains the different ultrasound features reported to be typical of adenomyosis. The link between the ultrasound features and histopathology has to be demonstrated and specified[27].

FIBROID (LEIOMYOMA)

A uterine fibroid is typically seen on ultrasound as a well-defined, round lesion within the myometrium or attached to it, often showing shadows at the edge of the lesion and/or internal fan-shaped shadowing (Figure 21). The echogenicity varies and some internal high echogenicity may be present. At color or power Doppler imaging, circumferential flow around the lesion is often visible.

However some fibroids do not exhibit such typical features. We suggest that such fibroids are labelled *sonographically atypical fibroids* (Figure 22).

On histological examination, fibroids are composed of smooth muscle cells and connective tissue in densely packed whorls. Acoustic shadows may arise from the interface between smooth muscle bundles, hyalinized connective tissue and normal myometrium[28]. The ultrasound appearances of a fibroid may depend on the proportion of muscle cells and fibrous stroma within the lesion.

VARIANTS OF FIBROIDS AND OTHER UTERINE SMOOTH MUSCLE TUMORS

VARIANTS OF FIBROIDS

Fibroids may undergo degeneration. This may be spontaneous or a result of induced infarction following uterine artery embolization. Coagulate necrosis is induced after high-intensity ultrasound or radio frequency ablation. Types of degeneration are: a) red, b) hyalin and c) cystic / myxoid (myxoid leiomyoma) or d) hydropic. Spontaneous degeneration may occur in pregnancy, and red degeneration is an initial manifestation[29] within days after infarction. The sonographic appearance of red degeneration may be unremarkable, although some cases of red degeneration have been reported as homogenous lesions with low echogenicity, a hyperechogenic rim and absent internal vascularity [30-32]. Hemorrhage and edema in these fibroids may give rise to tumors of mixed echogenicity. Late manifestations after infarction are most commonly hyaline degeneration[33;34].

Fibroids after induced infarction are often uniform, hypoechogenic, with a hyperechogenic rim with acoustic shadows[35;36]. There is usually no internal vascularity or at most a few disparate vessels. After spontaneous hyaline infarction fibroids may show mixed echogenicity or hypoechogenic cystic areas. Cystic or myxoid degeneration may

develop, resulting in regular hypoechogenic cystic areas with fluid or myxoid content[37;38]. Degeneration may also occur in malignant uterine smooth muscle tumors[39].

UTERINE SARCOMAS AND OTHER UTERINE SMOOTH MUSCLE TUMORS:

The prediction of malignancy is of utmost importance. However, data on the prediction of uterine sarcoma by ultrasound examination are scarce and mainly based on small retrospective case series, precluding definitive guidelines.

There are many rare uterine smooth muscle tumors other than benign leiomyomas[40], but only limited information on their ultrasound features has been reported to date. This issue has become increasingly important in view of the debate about when, or if, fibroids may be morcellated during laparoscopic surgery.

Malignant sarcomas comprise leiomyosarcoma (Figure 23), endometrial stromal sarcoma, adenosarcoma and undifferentiated sarcoma. Uterine sarcomas present as purely myometrial lesions and are typically single, large tumors[41]. Their ultrasound features may be indistinct from ordinary fibroids[42] or they may appear as an irregularly vascularized mass, with a regular or irregular outline often with irregular anechoic areas due to necrosis[43-49].

Uterine smooth muscle tumor of uncertain malignant potential (STUMP).

There are no specific ultrasound features described for STUMP. Intravenous leiomyomatosis, disseminated peritoneal leiomyomatosis and benign metastasizing leiomyoma[50-52] have the same ultrasound features as ordinary fibroids. There are often multiple fibroid and they may be recognized by their location outside uterine borders. These multiple fibroid should be distinguished from "diffuse leiomyomatosis"[53].

Fibroids **with little or no recurrent and/or metastatic potential:**

Ultrasound features of leiomyoma with bizarre nuclei (bizarre/symplastic/atypical leiomyoma); mitotically active leiomyoma; cellular and highly cellular leiomyoma; dissecting leiomyoma; leiomyoma with increased cellularity, no atypia nor mitotic figures and increased vascularity[40;54] may have the same macroscopically pathologic features as fibroids[40;54] and may have increased vascularity, as this feature seems to be related to cellularity[55].

A cotyledonoid leiomyoma or cotelydonoid dissecting leiomyoma[56-58] is a nodular tumor with placenta-like echogenicity at ultrasound, but it may also be cystic. Ultrasonographic features of lipoleiomyoma[59] comprise a hyperechogenic mass partly encased by a hypoechogenic rim. Ultrasonograpic features for epithelioid leiomyoma [40] and pallisading / neurilemoma-like leiomyoma[60] have not been described.

DISCUSSION

The terms and definitions presented in this paper aim to facilitate consistent reporting of myometrial lesions when using ultrasonography in both daily clinical practice and for research purposes. Clearly the clinical relevance of some of the terms that have been proposed have not yet been evaluated in prospective clinical studies. We acknowledge that some aspects of the systematic reporting we have suggested may require a relatively high level of ultrasound training. We also acknowledge that some of the proposed terms and definitions are too detailed for use in general clinical practice and will initially be suitable only for use in research settings. Future research should focus on the ability to predict specific pathologies and on the clinical relevance of the ultrasound features described in this paper. Although the members of panel involved in the writing of this consensus have different fields of expertise including gynecological ultrasonography, fertility treatment, hysteroscopy, general gynecology and clinical research, we acknowledge that they all come from Europe and the USA, leaving most of the areas of the world unrepresented.

The recent controversy about the safety of morcellation of lesions thought to be benign fibroids, but turning out to be malignant[5], highlights the importance of the reliable preoperative characterization of myometrial lesions. Although recognizing a typical fibroid on ultrasound is usually straightforward, differentiating between an atypical fibroid and a uterine sarcoma remains challenging. The establishment of an international database of ultrasound and Magnetic Resonance Imaging (MRI) images of uterine sarcomas and rare uterine tumors would be of great clinical value.

Adenomyosis may be difficult to diagnose with ultrasound. Different ultrasound features have been suggested to be associated with adenomyosis but at present it is not clear which are the minimal ultrasound criteria for diagnosis. Some features may carry a greater diagnostic weight than others[61] and the presence of more than one ultrasound feature associated with adenomyosis might increase the likelihood of the diagnosis[61-63]. We did not include the so called s-sign suggested to be typical of adenomyosis in our consensus statement, because this sign occurs when there is also deep infiltrative endometriosis in the posterior compartment[64].

The terms that we suggest to characterize the JZ are derived from MRI studies[20;30] . The JZ is better visualized by 3D[9;65] than by 2D ultrasound. The clinical implications of a thickened JZ or of JZ disruption according to ultrasound needs to be established [4;66].

The clinical relevance of myometrial lesions for abnormal uterine bleeding, pelvic pain, subfertility and pregnancy outcome is an important topic for research. Certain ultrasound features might prove to be more clinically relevant than others.

The role of a systematic evaluation of the ultrasound features of myometrial lesions when choosing management (expectant management, medical therapy, selective embolization, High-Intensity Focused Ultrasound or surgical treatment) and in the follow-up during or after treatment is another important topic for future research.

To conclude, the terms and definitions in this consensus statement enable clinicians to write a structured report when describing the ultrasound appearance of the myometrium and myometrial lesions and harmonize nomenclature for future research.

Acknowledgements

Tom Bourne is supported by the National Institute for Health Research (NIHR) Biomedical Research Centre based at Imperial College Healthcare NHS Trust and Imperial College London. The views expressed are those of the author(s) and not necessarily those of the NHS, the NIHR or the Department of Health.

Dirk Timmerman is Senior Clinical Investigator of Scientific Research Fund (FWO) Flanders.

References

1. Munro MG, Critchley HO, Fraser IS. The FIGO classification of causes of abnormal uterine bleeding in the reproductive years. *Fertil Steril* 2011; **95**:2204-8, 2208.

2. Munro MG, Critchley HO, Broder MS, Fraser IS. FIGO classification system (PALM-COEIN) for causes of abnormal uterine bleeding in nongravid women of reproductive age. *Int J Gynaecol Obstet* 2011; **113**:3-13.

3. Leone FP, Timmerman D, Bourne T, Valentin L, Epstein E, Goldstein SR, Marret H, Parsons AK, Gull B, Istre O, Sepulveda W, Ferrazzi E, Van den Bosch T. Terms, definitions and measurements to describe the sonographic features of the endometrium and intrauterine lesions: a consensus opinion from the International Endometrial Tumor Analysis (IETA) group. *Ultrasound Obstet Gynecol* 2010; **35**:103-112.

4. Gordts S, Brosens JJ, Fusi L, Benagiano G, Brosens I. Uterine adenomyosis: a need for uniform terminology and consensus classification. *Reprod Biomed Online* 2008; **17**:244-248.

5. Hampton T. Critics of fibroid removal procedure question risks it may pose for women with undetected uterine cancer. *JAMA* 2014; **311**:891-893.

6. Okaro E, Condous G, Khalid A, Timmerman D, Ameye L, Van Huffel SV, Bourne T. The use of ultrasound-based 'soft markers' for the prediction of pelvic pathology in women with chronic pelvic pain--can we reduce the need for laparoscopy? *BJOG* 2006; **113**:251-256.

7. Tetlow RL, Richmond I, Manton DJ, Greenman J, Turnbull LW, Killick SR. Histological analysis of the uterine junctional zone as seen by transvaginal ultrasound. *Ultrasound Obstet Gynecol* 1999; **14**:188-193.

8. Naftalin J, Jurkovic D. The endometrial-myometrial junction: a fresh look at a busy crossing. *Ultrasound Obstet Gynecol* 2009; **34**:1-11.

9. Exacoustos C, Brienza L, Di GA, Szabolcs B, Romanini ME, Zupi E, Arduini D. Adenomyosis: three-dimensional sonographic findings of the junctional zone and correlation with histology. *Ultrasound Obstet Gynecol* 2011; **37**:471-479.

10. Exacoustos C, Luciano D, Corbett B, De FG, Di FM, Luciano A, Zupi E. The uterine junctional zone: a 3-dimensional ultrasound study of patients with endometriosis. *Am J Obstet Gynecol* 2013; **209**:248-7.

11. Martins WP, Raine-Fenning NJ, Leite SP, Ferriani RA, Nastri CO. A standardized measurement technique may improve the reliability of measurements of endometrial thickness and volume. *Ultrasound Obstet Gynecol* 2011; **38**:107-115.

12. Woelfer B, Salim R, Banerjee S, Elson J, Regan L, Jurkovic D. Reproductive outcomes in women with congenital uterine anomalies detected by three-dimensional ultrasound screening. *Obstet Gynecol* 2001; **98**:1099-1103.

13. Abuhamad AZ, Singleton S, Zhao Y, Bocca S. The Z technique: an easy approach to the display of the mid-coronal plane of the uterus in volume sonography. *J Ultrasound Med* 2006; **25**:607-612.

14. Wamsteker K, Emanuel MH, de Kruif JH. Transcervical hysteroscopic resection of submucous fibroids for abnormal uterine bleeding: results regarding the degree of intramural extension. *Obstet Gynecol* 1993; **82**:736-740.

15. Casadio P, Youssef AM, Spagnolo E, Rizzo MA, Talamo MR, De AD, Marra E, Ghi T, Savelli L, Farina A, Pelusi G, Mazzon I. Should the myometrial free margin still be considered a limiting factor for hysteroscopic resection of submucous fibroids? A possible answer to an old question. *Fertil Steril* 2011; **95**:1764-1768.

16. Yang JH, Lin BL. Changes in myometrial thickness during hysteroscopic resection of deeply invasive submucous myomas. *J Am Assoc Gynecol Laparosc* 2001; **8**:501-505.

17. Timmerman D, Valentin L, Bourne TH, Collins WP, Verrelst H, Vergote I. Terms, definitions and measurements to describe the sonographic features of adnexal tumors: a consensus opinion from the International Ovarian Tumor Analysis (IOTA) Group. *Ultrasound Obstet Gynecol* 2000; **16**:500-505.

18. Alcazar JL. Three-dimensional power Doppler derived vascular indices: what are we measuring and how are we doing it? *Ultrasound Obstet Gynecol* 2008; **32**:485-487.

19. Raine-Fenning NJ, Campbell BK, Clewes JS, Kendall NR, Johnson IR. The reliability of virtual organ computer-aided analysis (VOCAL) for the semiquantification of ovarian, endometrial and subendometrial perfusion. *Ultrasound Obstet Gynecol* 2003; **22**:633-639.

20. Cucinella G, Billone V, Pitruzzella I, Lo Monte AI, Palumbo VD, Perino A. Adenomyotic cyst in a 25-year-old woman: case report. *J Minim Invasive Gynecol* 2013; **20**:894-898.

21. Ho ML, Ratts V, Merritt D. Adenomyotic cyst in an adolescent girl. *J Pediatr Adolesc Gynecol* 2009; **22**:33-38.

22. Protopapas A, Milingos S, Markaki S, Loutradis D, Haidopoulos D, Sotiropoulou M, Antsaklis A. Cystic uterine tumors. *Gynecol Obstet Invest* 2008; **65**:275-280.

23. Tahlan A, Nanda A, Mohan H. Uterine adenomyoma: a clinicopathologic review of 26 cases and a review of the literature. *Int J Gynecol Pathol* 2006; **25**:361-365.

24. Reinhold C, Tafazoli F, Mehio A, Wang L, Atri M, Siegelman ES, Rohoman L. Uterine adenomyosis: endovaginal US and MR imaging features with histopathologic correlation. *Radiographics* 1999; **19**:147-160.

25. Haines, Tailor. Obstetrics and Gynecologic pathology. Fourth edition ed. 1995.

26. Kishi Y, Suginami H, Kuramori R, Yabuta M, Suginami R, Taniguchi F. Four subtypes of adenomyosis assessed by magnetic resonance imaging and their specification. *Am J Obstet Gynecol* 2012; **207**:114-117.

27. Ferenczy A. Pathophysiology of adenomyosis. *Hum Reprod Update* 1998; **4**:312-322.

28. Kliewer MA, Hertzberg BS, George PY, McDonald JW, Bowie JD, Carroll BA. Acoustic shadowing from uterine leiomyomas: sonographic-pathologic correlation. *Radiology* 1995; **196**:99-102.

29. Ouyang DW, Economy KE, Norwitz ER. Obstetric complications of fibroids. *Obstet Gynecol Clin North Am* 2006; **33**:153-169.

30. Lev-Toaff AS, Coleman BG, Arger PH, Mintz MC, Arenson RL, Toaff ME. Leiomyomas in pregnancy: sonographic study. *Radiology* 1987; **164**:375-380.

31. Cooper NP, Okolo S. Fibroids in pregnancy--common but poorly understood. *Obstet Gynecol Surv* 2005; **60**:132-138.

32. Valentin L. Characterising acute gynaecological pathology with ultrasound: an overview and case examples. *Best Pract Res Clin Obstet Gynaecol* 2009; **23**:577-593.

33. McLucas B. Diagnosis, imaging and anatomical classification of uterine fibroids. *Best Pract Res Clin Obstet Gynaecol* 2008; **22**:627-642.

34. Ueda H, Togashi K, Konishi I, Kataoka ML, Koyama T, Fujiwara T, Kobayashi H, Fujii S, Konishi J. Unusual appearances of uterine leiomyomas: MR imaging findings and their histopathologic backgrounds. *Radiographics* 1999; **19**:131-145.

35. Nicholson TA, Pelage JP, Ettles DF. Fibroid calcification after uterine artery embolization: ultrasonographic appearance and pathology. *J Vasc Interv Radiol* 2001; **12**:443-446.

36. Allison SJ, Wolfman DJ. Sonographic Evaluation of Patients Treated with Uterine Artery Embolization. *Ultrasound Clinics* 2010; **5**:277-288.

37. Yarwood RL, Arroyo E. Cystic degeneration of a uterine leiomyoma masquerading as a postmenopausal ovarian cyst. A case report. *J Reprod Med* 1999; **44**:649-652.

38. Cohen JR, Luxman D, Sagi J, Jossiphov J, David MP. Ultrasonic "honeycomb" appearance of uterine submucous fibroids undergoing cystic degeneration. *J Clin Ultrasound* 1995; **23**:293-296.

39. Karpathiou G, Sivridis E, Giatromanolaki A. Myxoid leiomyosarcoma of the uterus: a diagnostic challenge. *Eur J Gynaecol Oncol* 2010; **31**:446-448.

40. Ip PP, Tse KY, Tam KF. Uterine smooth muscle tumors other than the ordinary leiomyomas and leiomyosarcomas: a review of selected variants with emphasis on recent advances and unusual morphology that may cause concern for malignancy. *Adv Anat Pathol* 2010; **17**:91-112.

41. Bonneau C, Thomassin-Naggara I, Dechoux S, Cortez A, Darai E, Rouzier R. Value of ultrasonography and magnetic resonance imaging for the characterization of uterine mesenchymal tumors. *Acta Obstet Gynecol Scand* 2013; **93**:261-268.

42. Jayakrishnan K, Koshy AK, Manjula P, Nair AM, Ramachandran A, Kattoor J. Endometrial stromal sarcoma mimicking a myoma. *Fertil Steril* 2009; **92**:1744-1746.

43. Exacoustos C, Romanini ME, Amadio A, Amoroso C, Szabolcs B, Zupi E, Arduini D. Can gray-scale and color Doppler sonography differentiate between uterine leiomyosarcoma and leiomyoma? *J Clin Ultrasound* 2007; **35**:449-457.

44. Aviram R, Ochshorn Y, Markovitch O, Fishman A, Cohen I, Altaras MM, Tepper R. Uterine sarcomas versus leiomyomas: gray-scale and Doppler sonographic findings. *J Clin Ultrasound* 2005; **33**:10-13.

45. Hata K, Hata T, Maruyama R, Hirai M. Uterine sarcoma: can it be differentiated from uterine leiomyoma with Doppler ultrasonography? A preliminary report. *Ultrasound Obstet Gynecol* 1997; **9**:101-104.

46. Seki K, Hoshihara T, Nagata I. Leiomyosarcoma of the uterus: ultrasonography and serum lactate dehydrogenase level. *Gynecol Obstet Invest* 1992; **33**:114-118.

47. Hata K, Hata T, Makihara K, Aoki S, Takamiya O, Kitao M, Harada Y, Nagaoka S. Sonographic findings of uterine leiomyosarcoma. *Gynecol Obstet Invest* 1990; **30**:242-245.

48. Szabo I, Szantho A, Csabay L, Csapo Z, Szirmai K, Papp Z. Color Doppler ultrasonography in the differentiation of uterine sarcomas from uterine leiomyomas. *Eur J Gynaecol Oncol* 2002; **23**:29-34.

49. Amant F, Coosemans A, Debiec-Rychter M, Timmerman D, Vergote I. Clinical management of uterine sarcomas. *Lancet Oncol* 2009; **10**:1188-1198.

50. Fasih N, Prasad Shanbhogue AK, Macdonald DB, Fraser-Hill MA, Papadatos D, Kielar AZ, Doherty GP, Walsh C, McInnes M, Atri M. Leiomyomas beyond the uterus: unusual locations, rare manifestations. *Radiographics* 2008; **28**:1931-1948.

51. Cohen DT, Oliva E, Hahn PF, Fuller AF, Jr., Lee SI. Uterine smooth-muscle tumors with unusual growth patterns: imaging with pathologic correlation. *AJR Am J Roentgenol* 2007; **188**:246-255.

52. Vaquero ME, Magrina JF, Leslie KO. Uterine smooth-muscle tumors with unusual growth patterns. *J Minim Invasive Gynecol* 2009; **16**:263-268.

53. Fedele L, Bianchi S, Zanconato G, Carinelli S, Berlanda N. Conservative treatment of diffuse uterine leiomyomatosis. *Fertil Steril* 2004; **82**:450-453.

54. Robboy SJ, Bentley RC, Butnor K, Anderson MC. Pathology and pathophysiology of uterine smooth-muscle tumors. *Environ Health Perspect* 2000; **108 Suppl 5**:779-784.

55. Minsart AF, Ntoutoume SF, Vandenhoute K, Jani J, Van PC. Does three-dimensional power Doppler ultrasound predict histopathological findings of uterine fibroids? A preliminary study. *Ultrasound Obstet Gynecol* 2012; **40**:714-720.

56. Smith CC, Gold MA, Wile G, Fadare O. Cotyledonoid dissecting leiomyoma of the uterus: a review of clinical, pathological, and radiological features. *Int J Surg Pathol* 2012; **20**:330-341.

57. Raga F, Sanz-Cortes M, Casan EM, Burgues O, Bonilla-Musoles F. Cotyledonoid dissecting leiomyoma of the uterus. *Fertil Steril* 2009; **91**:1269-1270.

58. Gurbuz A, Karateke A, Kabaca C, Arik H, Bilgic R. A case of cotyledonoid leiomyoma and review of the literature. *Int J Gynecol Cancer* 2005; **15**:1218-1221.

59. Prieto A, Crespo C, Pardo A, Docal I, Calzada J, Alonso P. Uterine lipoleiomyomas: US and CT findings. *Abdom Imaging* 2000; **25**:655-657.

60. Gisser SD, Young I. Neurilemoma-like uterine myomas:an ultrastructural reaffirmation of their non-Schwannian nature. *Am J Obstet Gynecol* 1977; **129**:389-392.

61. Dueholm M, Lundorf E, Hansen ES, Sorensen JS, Ledertoug S, Olesen F. Magnetic resonance imaging and transvaginal ultrasonography for the diagnosis of adenomyosis. *Fertil Steril* 2001; **76**:588-594.

62. Bazot M, Cortez A, Darai E, Rouger J, Chopier J, Antoine JM, Uzan S. Ultrasonography compared with magnetic resonance imaging for the diagnosis of adenomyosis: correlation with histopathology. *Hum Reprod* 2001; **16**:2427-2433.

63. Kepkep K, Tuncay YA, Goynumer G, Tutal E. Transvaginal sonography in the diagnosis of adenomyosis: which findings are most accurate? *Ultrasound Obstet Gynecol* 2007; **30**:341-345.

64. Di Donato N, Bertoldo V, Montanari G, Zannoni L, Caprara G, Seracchioli R. A simple sonographic sign associated to the presence of adenomyosis. *Ultrasound Obstet Gynecol* 2014;10.1002/uog.14750

65. Naftalin J, Hoo W, Nunes N, Mavrelos D, Nicks H, Jurkovic D. Inter- and intraobserver variability in three-dimensional ultrasound assessment of the endometrial-myometrial junction and factors affecting its visualization. *Ultrasound Obstet Gynecol* 2012; **39**:587-591.

66. Tocci A, Greco E, Ubaldi FM. Adenomyosis and 'endometrial-subendometrial myometrium unit disruption disease' are two different entities. *Reprod Biomed Online* 2008; **17**:281-291.

67. Dueholm M. Transvaginal ultrasound for diagnosis of adenomyosis: a review. *Best Pract Res Clin Obstet Gynaecol* 2006; **20**:569-582.

68. Reinhold C, Tafazoli F, Wang L. Imaging features of adenomyosis. *Hum Reprod Update* 1998; **4**:337-349.

69. Chiang CH, Chang MY, Hsu JJ, Chiu TH, Lee KF, Hsieh TT, Soong YK. Tumor vascular pattern and blood flow impedance in the differential diagnosis of leiomyoma and adenomyosis by color Doppler sonography. *J Assist Reprod Genet* 1999; **16**:268-275.

Myometrium paper: TABLES

Table 1: Reporting the myometrium

Table 2: Reporting the Junctional Zone (JZ)

Table 3: Reporting the vascularity of the myometrium

Table 4: Reporting the myometrium in general clinical practice

Table 5: Features considered important in the diagnosis of fibroids and adenomyosis.

Table 1: Reporting the myometrium

TABLE 1: REPORTING THE MYOMETRIUM.			
FEATURE TO BE DESCRIBED		**DESCRIPTION/TERM**	**QUANTIFICATION/MEASUREMENT**
Uterine corpus (Fig. 1)		*Length, antero-posterior diameter, transverse diameter, volume*	Length =([fundus] + [cavity]) *(d1),* antero-posterior diameter *(d2),* transverse diameter *(d3)* , V *(cm^3)= d1 cm × d2 cm × d3 cm × 0.523*
Uterus corpus and cervix (Fig. 1)			Total length = [fundus] + [cavity] + [cervix] = d1 + c
Serosal contour (Fig. 2a+b)		Regular / lobulated	
MYOMETRIUM			
Myometrial walls (Fig. 2b)		Symmetrical / asymmetrical	Ratio or subjective impression of asymmetry
Overall echogenicity		Homogeneous / heterogeneous	
MYOMETRIAL LESIONS		Well defined / ill defined	
	Number		Exact number: n
	Location*	Location: anterior, posterior, fundal, right lateral or left lateral, global	
	Site (Fig. 7)*	Site (for well-defined lesions): FIGO-classification 1-7	
	Size*		Three perpendicular diameters (a1,a2,a3), and/or Volume (V) V cm^3=a1 cm × a2 cm × a3 cm × 0.523
	Outer lesion free margin (OFM) (Fig. 8)		The minimal distance between the serosal surface and the outermost border of the lesion
	Inner lesion free margin (IFM) (Fig. 8)		The minimal distance between the endometrium and the inner border of the lesion
	Penetration of ill-defined lesions (Fig. 9)	Ratio between thickness of lesion and the total uterine wall thickness, measured on the same image	Penetration = maximal diameter of the lesion perpendicular to the endometrium / maximal wall thickness perpendicular to the endometrium
Extent of ill-defined lesions		Localized (< 50% of total uterine volume involved) or diffuse (≥ 50% of total uterine volume involved)	% of myometrium volume involved
Echogenicity (Fig. 10a, Fig. 10b)		Uniform: hypo-, iso-, hyper-echogenic Non- uniform: mixed echogenicity, cystic areas (regular/irregular); anechogenic, low level, ground glass, mixed echogenicity of cyst fluid	Very hypoechogenic - -, hypoechogenic-, isoechogenic, hyperechogenic+, very hyperechogenic ++
Rim (Fig. 11)		Hypo- or hyper-echogenic, or ill-defined	
Shape (Fig. 11)		Round / Not round: oval, lobulated, irregular	
Shadowing (Fig. 12a)	Edge shadows	Present / Absent	Degree of shadowing: slight, moderate, strong
	Internal shadows	Present / Absent	Degree of shadowing: slight, moderate, strong
	Fan shaped shadowing (Fig. 12b)	Present / Absent	Degree of shadowing: slight, moderate, strong
Cysts (Fig. 13a)		Present / Absent	
	Size		Maximum diameter of largest cyst
	Number of cysts		Exact number or (single, 1-5, >5)
	Echogenicity	Cyst fluid: anechogenic, low level, ground glass, mixed echogenicity Hyperechogenic rim: Present/Absent	
Hyperechogenic islands (Fig. 13b)		Present/Absent	
	Outline	Regular, irregular or ill defined	
	Size		Maximum diameter
	Number		Exact number or (single, 1-5, >5)
Subendometrial echogenic lines & buds (Fig. 14)		Present/Absent	
	Number		Exact number or (single, 1-5, >5) Location

Definitions of the terms and their quantifications are described in the text and illustrated by ultrasound images and schematic drawings. Those with a white background are items of importance in daily clinical practice; while items on a shaded background are of interest for research purposes. Measurements are reported in mm or cm (to tenths of a cm).* if clinically relevant (e.g. preoperative workup before myomectomy)

Table 2: Reporting the Junctional Zone (JZ)

TABLE 2: REPORTING THE JUNCTIONAL ZONE		
STRUCTURE TO BE DESCRIBED	**DESCRIPTION**	**MEASUREMENT**
Junctional zone	Regular / irregular / interrupted / not visible / not assessable	maximum JZ thickness (JZ_{max}) in mm minimal JZ thickness(JZ_{min}) in mm or ratio JZ/ total myometrial wall thickness
Irregular or interrupted junctional zone	Location: anterior, posterior, fundus, lateral right, lateral left, or global	Magnitude of irregularity: (JZ_{max}) - (JZ_{min}) = JZ_{dif} Extent of irregularity: % of JZ being irregular (< 50% or $\geq$ 50%)
Interrupted junctional zone	Location: anterior, posterior, fundus, lateral right, lateral left, or global	Interruption of JZ: % of JZ not visualized (< 50% or $\geq$ 50%)
Irregularity of JZ	Cystic areas, hyperechogenic dots, hyperechogenic buds and lines (in each location)	

Definition of the terms and their quantifications are described in the text and illustrated by ultrasound images and schematic drawings (Figure 5 and 6). With a white background are items of importance in daily clinical practice, while items on a shaded background are of interest for research purposes.

Table 3: Reporting the vascularity of the myometrium

TABLE 3: REPORTING THE VASCULARITY OF THE MYOMETRIUM		
Vascularization to be assessed	**DESCRIPTION**	**MEASUREMENT**
Whole uterus		
Overall vessel pattern (Fig. 16)	Uniform / non-uniform	
Lesions		
Amount of color (in a lesion) (Fig. 18)	Color score (both the percentage of the lesion being vascularized and the color hue are taken into account)	no color (1); minimal color (2); moderate color (3); abundant color (4)
In case of uneven spread of vascularization	Color score in most vascularized part	no color (1); minimal color (2); moderate color (3); abundant color (4)
	Percent of solid tissue with color signal	0-100%
	Compared to adjacent myometrium	Iso-, hypo-, or hyper-vascularity
Location of vessels (Fig. 16, 17)	Circumferential / intra-lesional Uniform /not uniform (areas with increased / decreased vascularity)	
Vessel morphology (Fig. 16, 19)	Number: single / multiple Size: large and equal / small and equal / unequal Branching: regular, irregular, no branching Direction: perpendicular, not perpendicular	

Items with a white background are of importance in daily clinical practice; while items on a shaded background are of interest for research purposes.

Table 4: Reporting the myometrium in general clinical practice

FEATURE TO BE DESCRIBED		DESCRIPTION/TERM
UTERINE CORPUS		Length, antero-posterior diameter, transverse diameter
Myometrial walls		Symmetrical / asymmetrical
Overall echogenicity		Homogeneous / heterogeneous
MYOMETRIAL LESIONS		Well defined / ill defined
	Number	Number (1, 2, 3 or estimation in case > 4 lesions)
	Location	Location of the largest/clinically relevant lesion(s): anterior, posterior, fundal, right lateral or left lateral, global
	Site	Site (for well-defined lesions) of the largest/clinically relevant lesion(s): FIGO-classification 1-7
	Size	The maximal diameter of the largest/clinically relevant lesion(s)
Shadowing	Edge shadows	Present / Absent
	Internal shadows	Present / Absent
	Fan shaped shadowing	Present / Absent
Cysts		Present / Absent
Hyperechogenic islands		Present / Absent
Subendometrial echogenic lines & buds		Present / Absent
JUNCTIONAL ZONE		Regular / Poorly defined
VASCULARITY OF THE MYOMETRIUM		
Overall vessel pattern (in the whole uterus)		Uniform / non-uniform
Amount of color (in a lesion)	Color score	(1) no color; (2) minimal color; (3) moderate color; (4) abundant color

Table 5: Features considered important in the diagnosis of fibroids and adenomyosis.

TABLE 4: Features considered important in the diagnosis of fibroids and adenomyosis.		
FEATURE	**TYPICAL FIBROID**	**ADENOMYOSIS**
Serosal contour of the uterus	lobulated or regular	often globally enlarged uterus
Definition of lesion	well-defined	ill-defined in diffuse adenomyosis (adenomyoma may be well-defined)
Symmetry of uterine walls	asymmetrical in the presence of well-defined lesion(s)	myometrial anterior-posterior asymmetry
LESION		
Outline	well-defined	ill-defined
Shape	round, oval, lobulated	ill-defined
Contour	smooth	irregular or ill-defined
Rim	hypo- or hyper-echogenic	no rim
Shadowing	edge shadows internal shadows (often fan shaped shadowing)	no edge shadows fan shaped shadowing[67]
Echogenicity	uniform: hyper- / iso- / hypo-echogenic non-uniform: mixed echogenicity	non-uniform: mixed echogenicity[67,68] cysts[20-24;62], hyper-echogenic islands, subendometrial lines and buds[24;63]
Vascularity	circumferential flow	translesional flow[69]
JUNCTIONAL ZONE (JZ)		
JZ-thickness, regularity	not-thickened, regular or not visible	thickened irregular or ill- defined[9;61-63]
JZ interruption	interrupted or overstretched junctional zone in areas with lesions of FIGO type 1-3 (Fig. 7)	interrupted junctional zone (even in absence of localized lesions)[9]

Myometrium paper: FIGURES

Figure 1: Measurement of the uterus.

Figure 1. *Schematic drawings showing how to measure the uterus. The total length of the uterine corpus (d1) is the sum of the fundus length (a) and the cavity length (b): [d1 = a + b]; AP is the largest antero-posterior diameter (d2); T is the largest transverse diameter (d3). The total length of the uterus is the sum of the corpus (d1) and the cervix length (c). The volume (cm3) of the corpus uteri is calculated as d1(cm) x d2(cm) x d3(cm) x 0.523*

Figure 2: The serosal contour of the uterus

Figure 2. *Schematic drawings illustrating how to describe the serosal contour of the uterus. The serosal contour of the uterus may be regular (upper row) or lobulated (lower row). The definition of a regular uterus is a normal uterus without any myometrial lesions, a uterus with an intramural lesion that does not alter the normal smooth serosal contour of the uterus (yellow arrow). Regular uterus includes for example an asymmetrical uterus (green arrows highlight the thickness of the anterior and posterior myometrial walls) or a globally enlarged uterus (illustrated by dotted line arrows in the upper row of images).*

Figure 3: Symmetry of the uterine walls

Figure 3. *Schematic drawings illustrating the symmetry of the uterine walls. Symmetrical walls are shown in the upper row and asymmetrical walls in the lower row.*

Figure 4: Junctional zone on 3D-ultrasound imaging

Figure 4. *Multiplanar view of the uterine corpus obtained by three-dimensional ultrasound. The junctional zone (JZ) can be seen as a dark line just beneath the endometrium (green arrow, and yellow dotted line).The JZ of the anterior and posterior wall is visualized in the A and B plane (upper row left and right), the JZ of the left and right lateral wall and of the fundus in the C plane (lower row).*

Figure 5: Junctional zone

Figure 5*. These schematic drawings illustrate regular, irregular, interrupted and not visible junctional zone (JZ) displayed in the coronal plane (images to the left) and in the sagittal plane (images to the right).*

Figure 6: Measurement of the junctional zone (for research purposes)

Figure 6: *Schematic drawings and ultrasound images illustrating measurement of junctional zone (JZ) thickness. Measurement of JZ_{max} and JZ_{min} is illustrated in the schematic drawings (first row, red arrows). JZ_{max} is the thickness of the JZ where it appears to be at its thickest and JZ_{min} is where the JZ appears to be at its thinnest after evaluation of the total three-dimensional volume of the uterus. The total wall thickness (yellow arrow) is measured at the site where the JZ is measured to calculate the ratio JZ/total wall thickness. The total wall thickness includes the JZ.*

In the two-dimensional image (lower row left) the JZ is measured where it appears at its thickest (red arrows). In the coronal view (C-plane) of the uterus (lower row right) the JZ_{max} in the right lateral wall is marked (yellow calipers).

Figure 7: The FIGO classification of myomas

Figure 7: *The FIGO classification of myomas (Adapted from: Munro MG et al [2]) should be used to report the* ***site*** *of well-defined localized lesions:* 0 = pedunculated intracavitary; 1 = submucosal <50% intramural; 2 = submucosal ≥50% intramural; 3 = 100% intramural, but contacts the endometrium; 4 = intramural; 5 = subserosal ≥50% intramural; 6 = subserosal <50% intramural; 7 = subserosal pedunculated; 8 = other (e.g. cervical, parasitic)[1;15]

Figure 8: Schematic drawings illustrating the measurement of the inner lesion free margin (IFM) (green arrow and dotted line) and of the outer lesion free margin (OFM) (yellow arrow and dotted line) of a lesion

Figure 9: Penetration (for research purposes)

Figure 9: *Penetration is defined as the ratio between the maximal thickness of the lesion (yellow arrow) and the total uterine wall thickness (red arrow). Both measurements are taken perpendicular to the endometrium on the same ultrasound image. The penetration is measured where the lesion appears to be at its largest. Although the images illustrate sagittal sections through the uterus the measurements to calculate penetration can be taken in any plane.*

Figure 10a: Lesion echogenicity

Figure 10a. *Schematic drawings and ultrasound images illustrating different types of lesion echogenicity. The echogenicity of a lesion may be uniform (hypo-, iso- or hyper-echogenic) or non-uniform with mixed echogenicity, echogenic areas, or cystic areas.*

Figure 10b. Echogenicity of a uniform lesion (for research purposes)

Figure 10b. *The mean grey-tone of a lesion may be compared to the adjacent myometrium and classified as hypo-, iso- or hyper-echogenic. Echogenicity may be scored as very hypoechogenic (- -), hypoechogenic (-), isoechogenic, hyperechogenic (+) or very hyperechogenic (++).*

Figure 11. Rim and shape of myometrial lesions

Figure 11. *Schematic drawings illustrating the rim and shape of myometrial lesions. The **rim** of a myometrial lesion may be hypo- or hyper-echogenic or ill-defined and its **shape** may be round or not round, e.g. oval shaped, lobulated or irregular.*

Figure 12: Shadowing

Figure 12a. *Schematic (upper row) and ultrasound images (lower row) illustrating edge shadowing and internal shadowing. Ultrasound pictures illustrate edge shadows (yellow arrow) and internal shadows (green arrow).*

Figure 12b. All ultrasound images illustrating fan shaped shadowing. The image in the lower row also shows an anechogenic myometrial cyst with a hyperechogenic rim surrounding the cyst and acoustic enhancement posterior to the cyst.

Figure 13a-c: Ultrasound images showing a) myometrial cysts (yellow arrow) b) hyperechogenic islands (surrounded by green dotted lines), and c) echogenic spots (yellow arrows).

Figure 14: Ultrasound images illustrating echogenic subendometrial lines and buds. The lines and buds are encircled by green dotted lines.

Figure 15: Normal vascular pattern of the myometrium

Figure 15: *Schematic drawings (upper row) and ultrasound images (lower rows) illustrating the normal vascular pattern of the myometrium. The arcuate vessels of the uterus are visible at the periphery of the myometrium, parallel to the uterine serosa. Perpendicular to the arcuate vessels, the radial arteries and veins flowing throughout the myometrium are usually detectable.*

Figure 16: Vascular pattern within the myometrium

Figure 16. Schematic and ultrasound images illustrating the vascular pattern within the myometrium and in myometrial lesions. The vascular pattern of the myometrium may be uniform (upper row) or non-uniform (middle row). The vascular pattern of a myometrial lesion may be circumferential, intra-lesional or both circumferential and intra-lesional (lower row).

Figure 17: Translesional vascularity

Figure 17*. Ultrasound images and a schematic drawing illustrating translesional vascularity which is defined as vessels perpendicular to the endometrium crossing the lesion.*

Figure 18: Color score of circumferential and intra-lesional vascularity.

Figure 18. *Schematic images illustrating the color score (amount of color Doppler signals) in the circumference of and inside myometrial lesions. The amount of color is estimated subjectively. The color score is based on the subjective evaluation of both the percentage of the lesion being vascularized and the color hue. A color score of 1 represents no color, 2 minimal amount of color, 3 moderate and 4 abundant amount of color.*

Figure 19: Vascularization of a myometrial lesion: vessel number, size, branching and direction (for research purposes)

Figure 19. *Schematic drawings illustrating how to describe the vascularization of a myometrial lesion in clinical research, in terms of vessel number, vessel size (depending on the research protocol the vessel diameter may be measured), vessel branching and vessel direction. Circumferential vessels are the vessels surrounding a lesion.*

Figure 20: Schematic drawings illustrating the ultrasound features currently considered to be typical of adenomyosis.

Figure 21: Schematic drawings illustrating the ultrasound features currently considered to be typical of uterine fibroids.

Figure 22: Ultrasound images showing fibroids with atypical sonographic features. These fibroid have a non-uniform echogenicity, intralesional anechoic cysts and some have areas with hyperechogenicity. There is an irregular outline of the FIGO type1 fibroid (lower right).

Figure 23: Gray scale and color Doppler images of a sarcoma in the anterior wall of the uterus. The uterine corpus (yellow arrows) is located posteriorly and contains clear fluid (green arrow).

Myometrium paper: FIGURES

Figure 1: Measurement of the uterus.

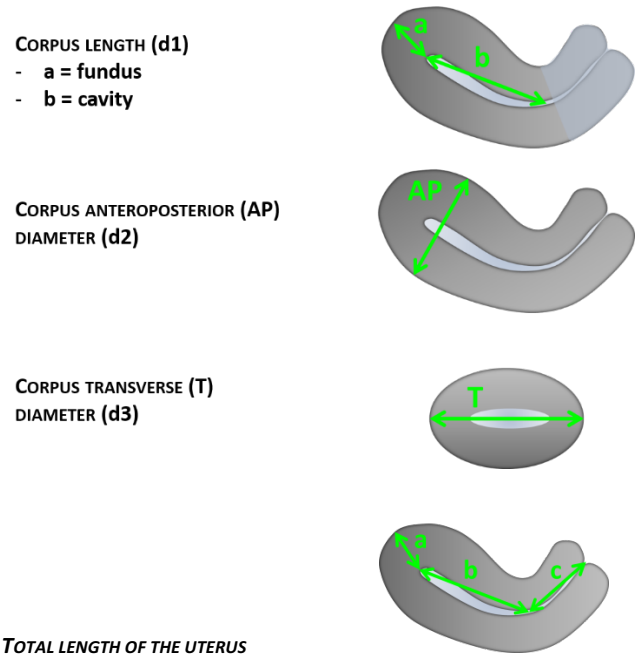

Figure 1. *Schematic drawings showing how to measure the uterus. The total length of the uterine corpus (d1) is the sum of the fundus length (a) and the cavity length (b): [d1 = a + b]; AP is the largest antero-posterior diameter (d2); T is the largest transverse diameter (d3). The total length of the uterus is the sum of the corpus (d1) and the cervix length (c). The volume (cm3) of the corpus uteri is calculated as d1(cm) x d2(cm)x d3(cm) x 0.523*

Figure 2: The serosal contour of the uterus

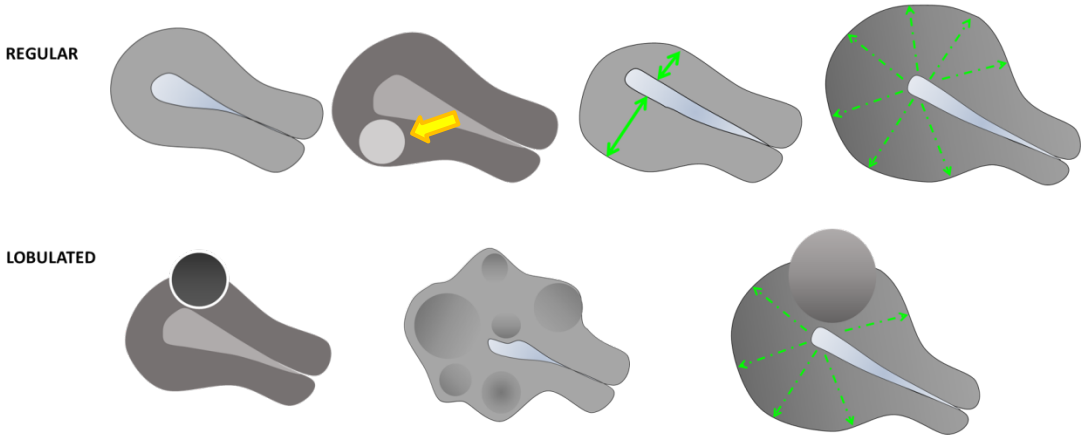

Figure 2. *Schematic drawings illustrating how to describe the serosal contour of the uterus. The serosal contour of the uterus may be regular (upper row) or lobulated (lower row). The definition of a regular uterus is a normal uterus without any myometrial lesions, a uterus with an intramural lesion that does not alter the normal smooth serosal contour of the uterus (yellow arrow). Regular uterus includes for example an asymmetrical uterus (green arrows highlight the thickness of the anterior and posterior myometrial walls) or a globally enlarged uterus (illustrated by dotted line arrows in the upper row of images).*

Figure 3: Symmetry of the uterine walls

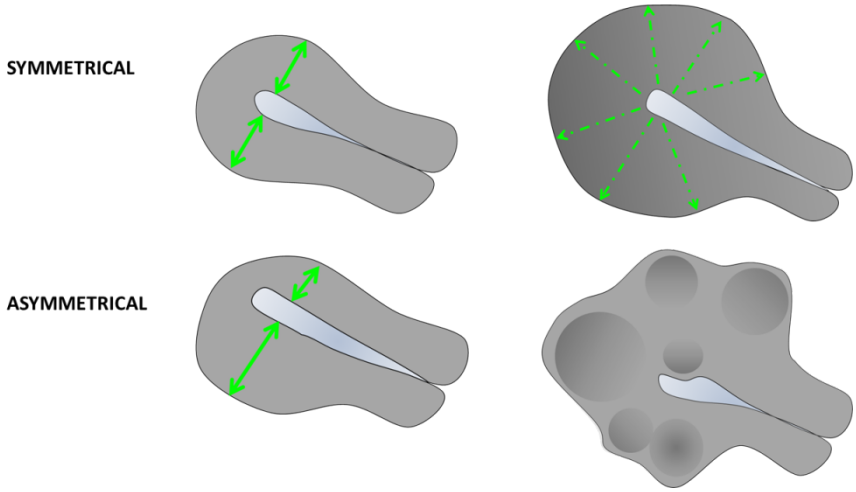

Figure 3. *Schematic drawings illustrating the symmetry of the uterine walls. Symmetrical walls are shown in the upper row and asymmetrical walls in the lower row.*

Figure 4: Junctional zone on 3D-ultrasound imaging

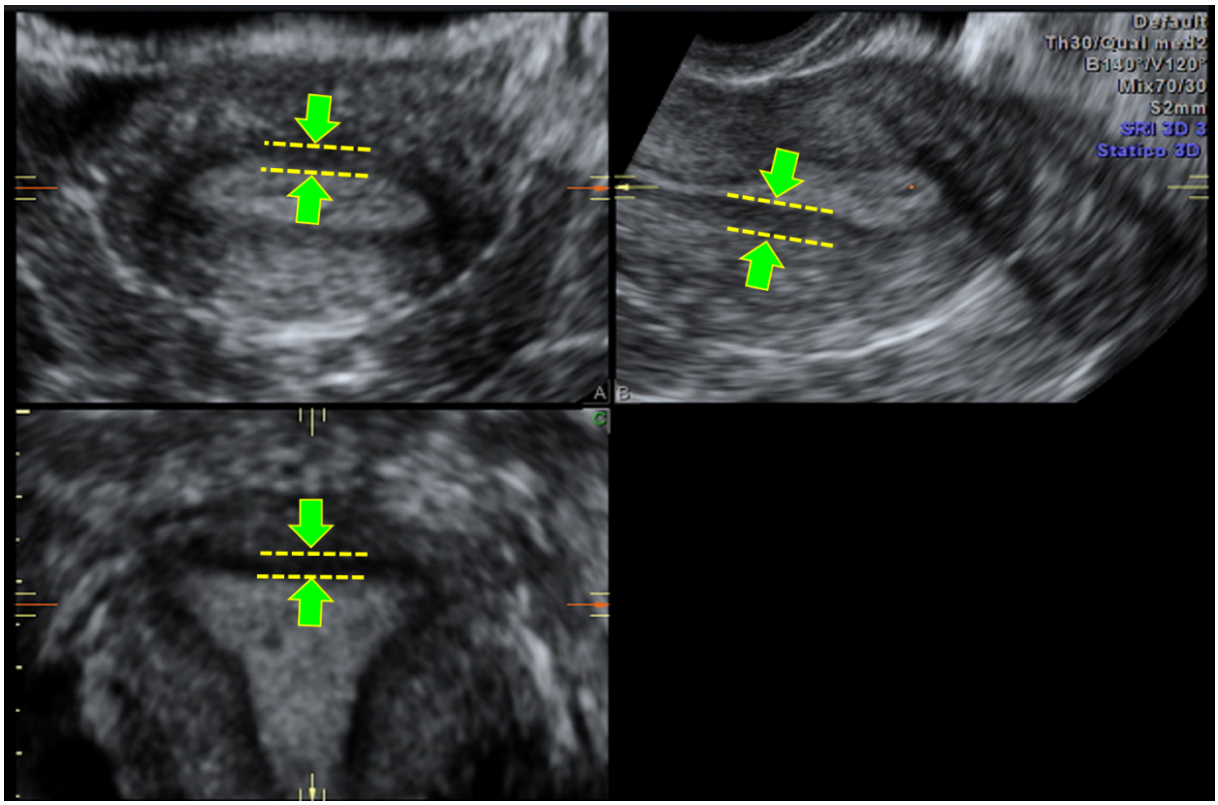

Figure 4. *Multiplanar view of the uterine corpus obtained by three-dimensional ultrasound. The junctional zone (JZ) can be seen as a dark line just beneath the endometrium (green arrow, and yellow dotted line).The JZ of the anterior and posterior wall is visualized in the A and B plane (upper row left and right), the JZ of the left and right lateral wall and of the fundus in the C plane (lower row).*

Figure 5: Junctional zone

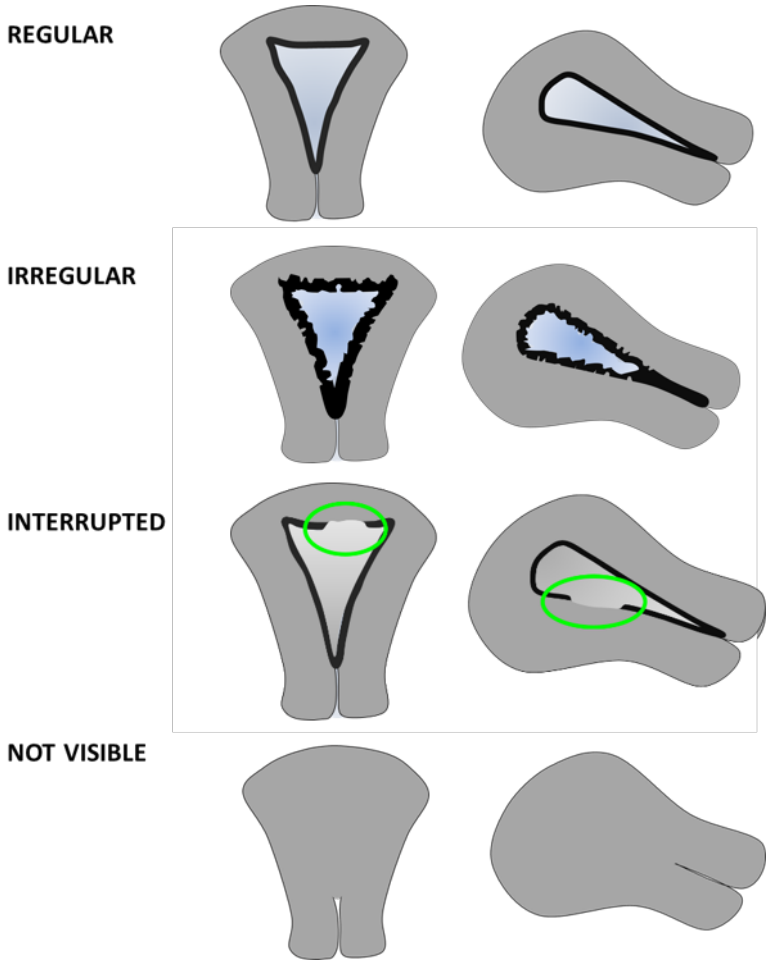

Figure 5*. These schematic drawings illustrate regular, irregular, interrupted and not visible junctional zone (JZ) displayed in the coronal plane (images to the left) and in the sagittal plane (images to the right).*

Figure 6: Measurement of the junctional zone (for research purposes)

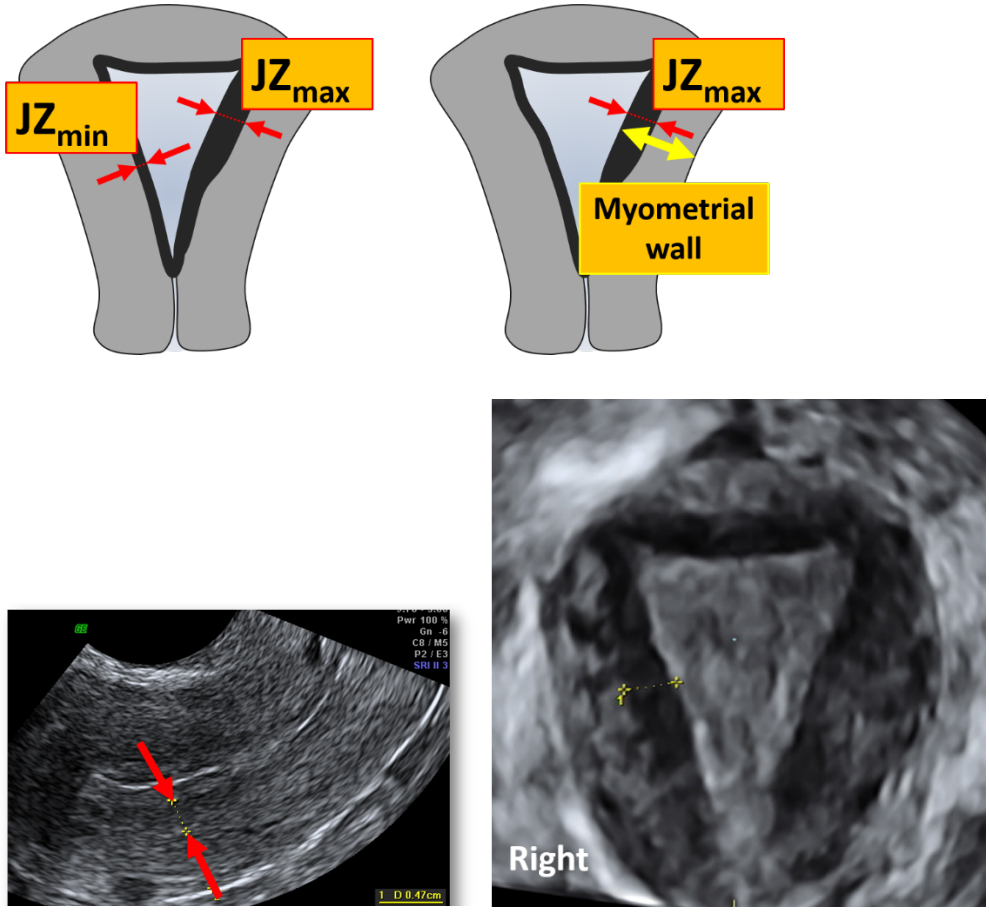

Figure 6: *Schematic drawings and ultrasound images illustrating measurement of junctional zone (JZ) thickness. Measurement of JZ_{max} and JZ_{min} is illustrated in the schematic drawings (first row, red arrows). JZ_{max} is the thickness of the JZ where it appears to be at its thickest and JZ_{min} is where the JZ appears to be at its thinnest after evaluation of the total three-dimensional volume of the uterus. The total wall thickness (yellow arrow) is measured at the site where the JZ is measured to calculate the ratio JZ/total wall thickness. The total wall thickness includes the JZ.*

In the two-dimensional image (lower row left) the JZ is measured where it appears at its thickest (red arrows). In the coronal view (C-plane) of the uterus (lower row right) the JZ_{max} in the right lateral wall is marked (yellow calipers).

Figure 7: The FIGO classification of myomas

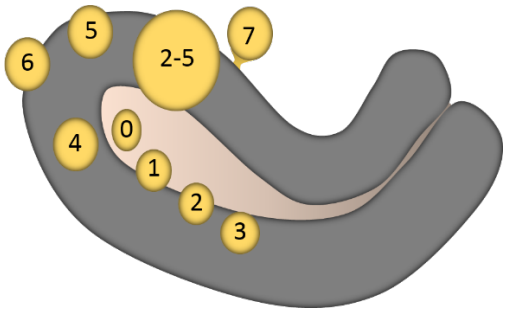

Figure 7: *The FIGO classification of myomas (Adapted from: Munro MG et al [2]) should be used to report the* ***site*** *of well-defined localized lesions:* 0 = pedunculated intracavitary; 1 = submucosal <50% intramural; 2 = submucosal ≥50% intramural; 3 = 100% intramural, but contacts the endometrium; 4 = intramural; 5 = subserosal ≥50% intramural; 6 = subserosal <50% intramural; 7 = subserosal pedunculated; 8 = other (e.g. cervical, parasitic)[1;15]

Figure 8: Schematic drawings illustrating the measurement of the inner lesion free margin (IFM) (green arrow and dotted line) and of the outer lesion free margin (OFM) (yellow arrow and dotted line) of a lesion

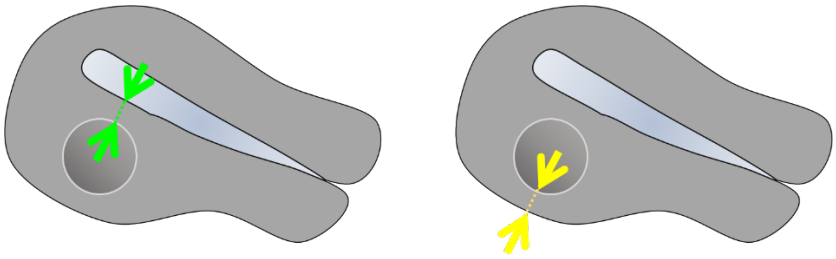

Figure 9: Penetration (for research purposes)

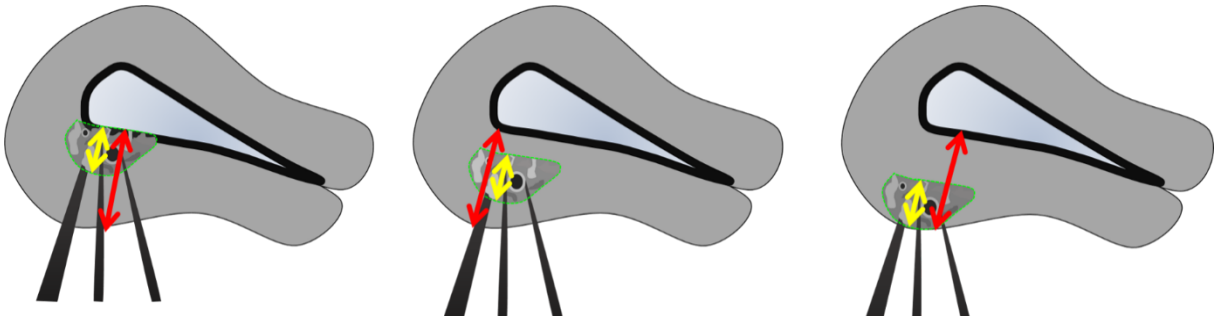

Figure 9: *Penetration is defined as the ratio between the maximal thickness of the lesion (yellow arrow) and the total uterine wall thickness (red arrow). Both measurements are taken perpendicular to the endometrium on the same ultrasound image. The penetration is measured where the lesion appears to be at its largest. Although the images illustrate sagittal sections through the uterus the measurements to calculate penetration can be taken in any plane.*

Figure 10a: Lesion echogenicity

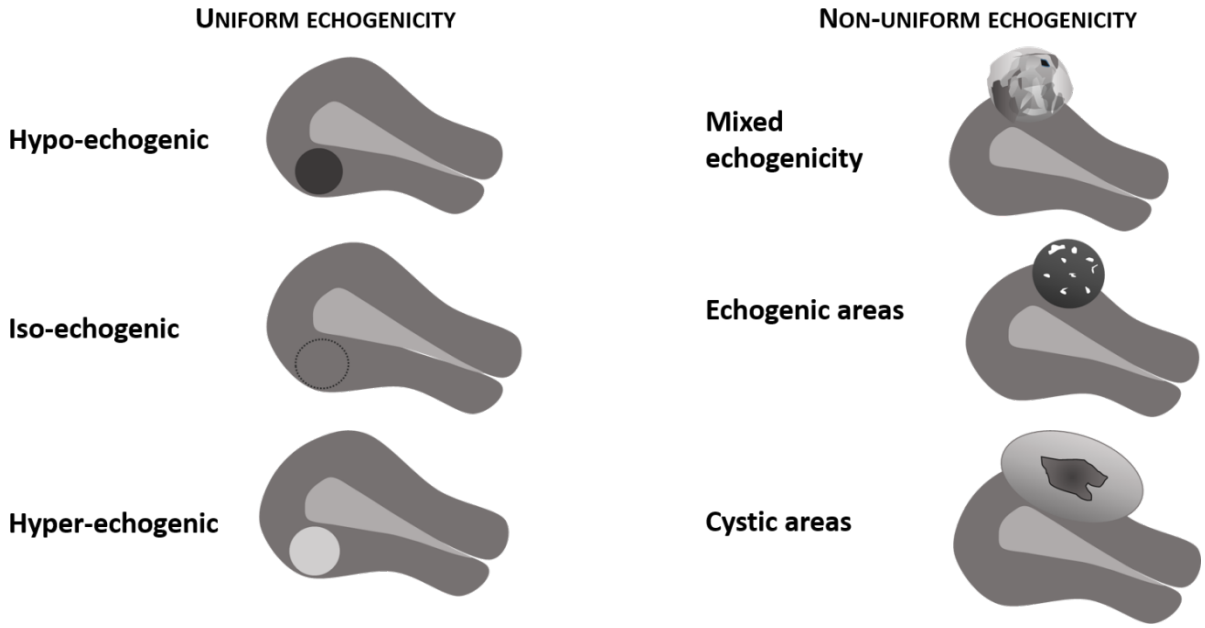

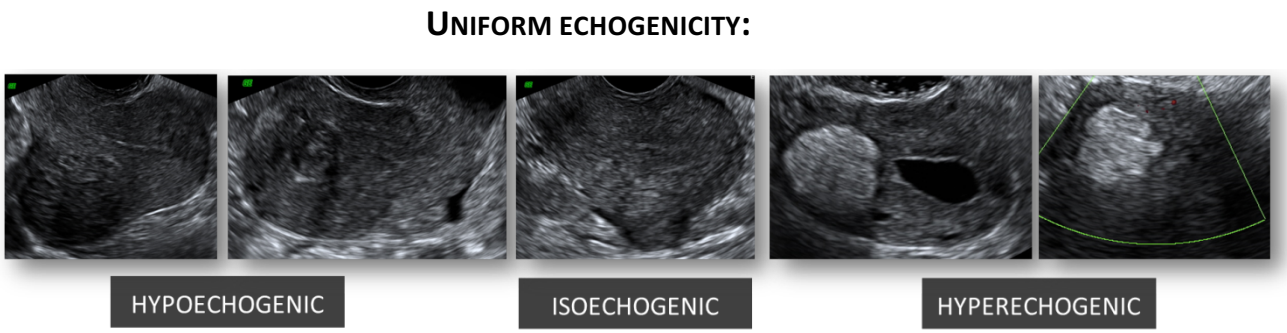

Figure 10a. *Schematic drawings and ultrasound images illustrating different types of lesion echogenicity. The echogenicity of a lesion may be uniform (hypo-, iso- or hyper-echogenic) or non-uniform with mixed echogenicity, echogenic areas, or cystic areas.*

Figure 10b. Echogenicity of a uniform lesion (for research purposes)

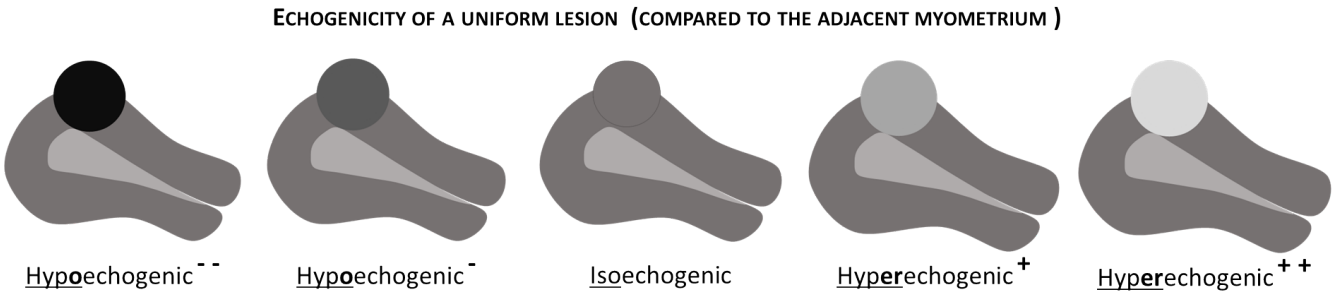

Figure 10b. *The mean grey-tone of a lesion may be compared to the adjacent myometrium and classified as hypo-, iso- or hyper-echogenic. Echogenicity may be scored as very hypoechogenic (- -), hypoechogenic (-), isoechogenic, hyperechogenic (+) or very hyperechogenic (++).*

Figure 11. Rim and shape of myometrial lesions

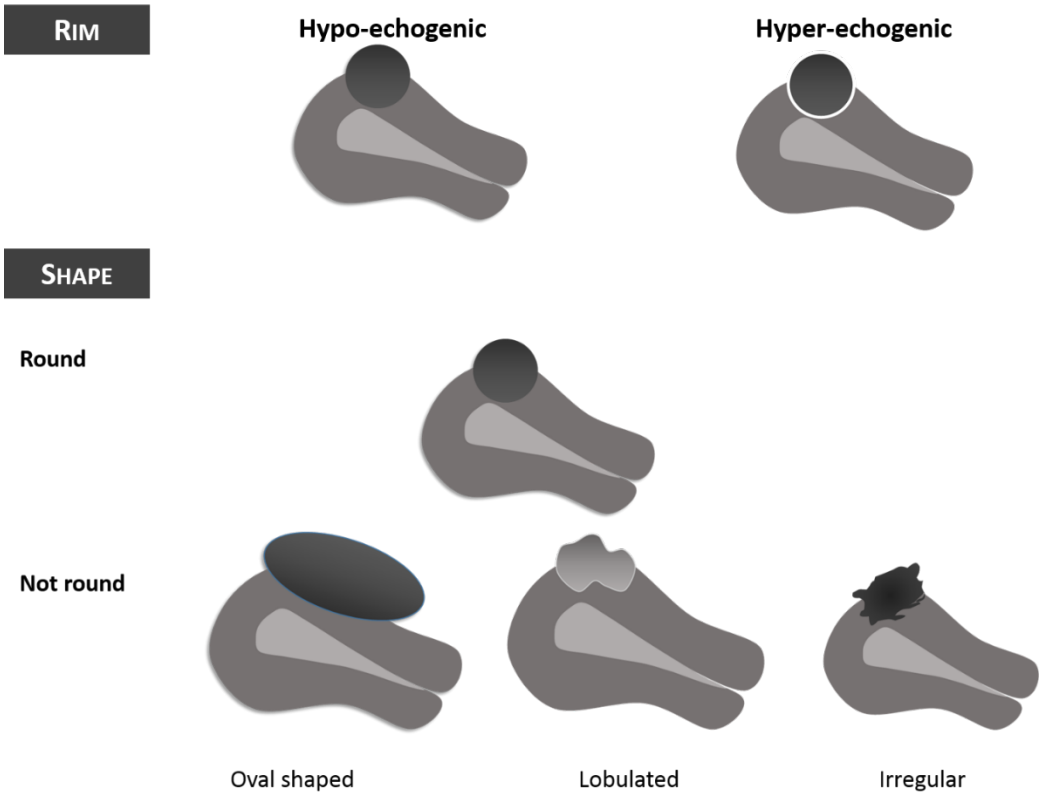

Figure 11. *Schematic drawings illustrating the rim and shape of myometrial lesions. The* ***rim*** *of a myometrial lesion may be hypo- or hyper-echogenic or ill-defined and its* ***shape*** *may be round or not round, e.g. oval shaped, lobulated or irregular.*

Figure 12a: Shadowing

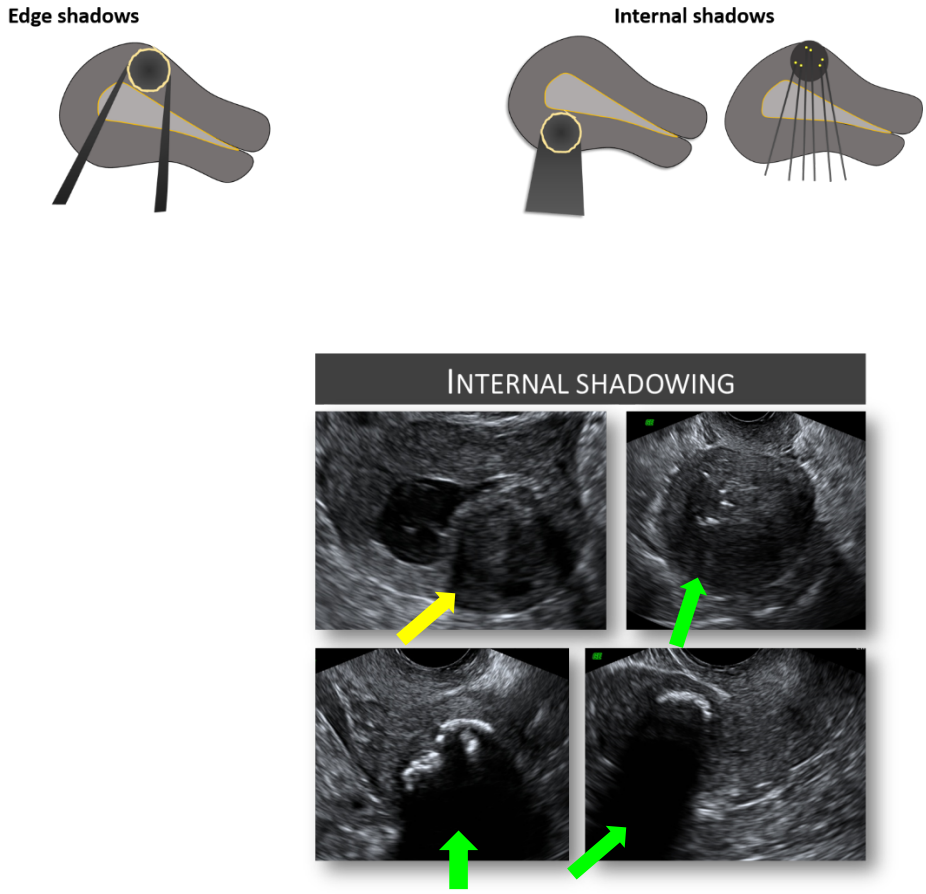

Figure 12a. *Schematic (upper row) and ultrasound images (lower row) illustrating edge shadowing and internal shadowing. Ultrasound pictures illustrate edge shadows (yellow arrow) and internal shadows (green arrow).*

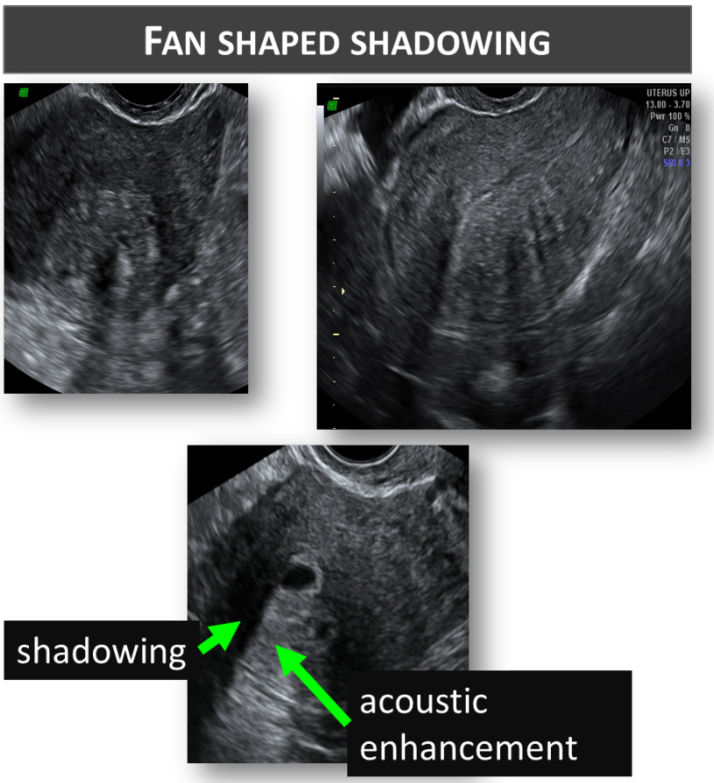

Figure 12b.All ultrasound images illustrating fan shaped shadowing. The image in the lower row also shows an anechogenic myometrial cyst with a hyperechogenic rim surrounding the cyst and acoustic enhancement posterior to the cyst.

Figure 13a-c: Ultrasound images showing a) myometrial cysts (yellow arrow) b) hyperechogenic islands (surrounded by green dotted lines), and c) echogenic spots (yellow arrows).

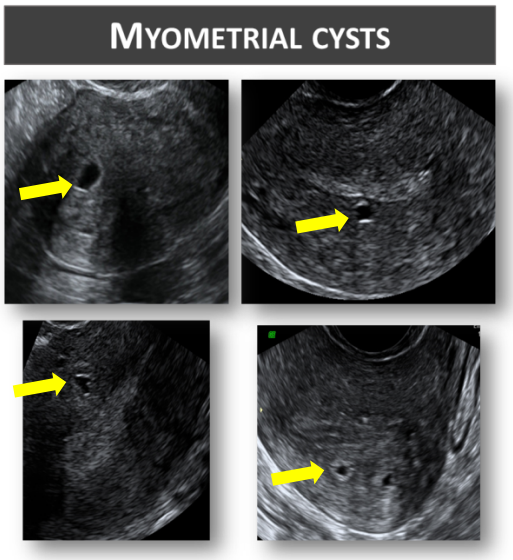

13a

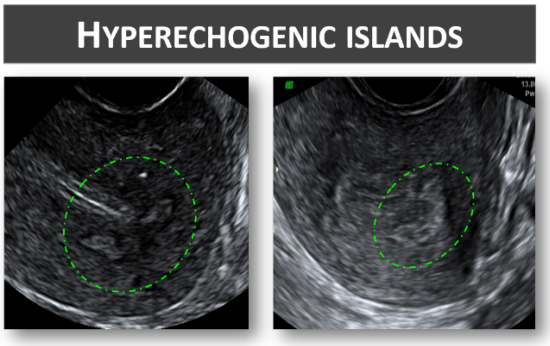

13b

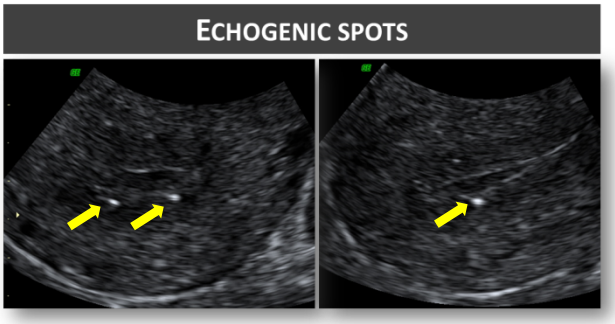

13c

Figure 14: Ultrasound images illustrating echogenic subendometrial lines and buds. The lines and buds are encircled by green dotted lines.

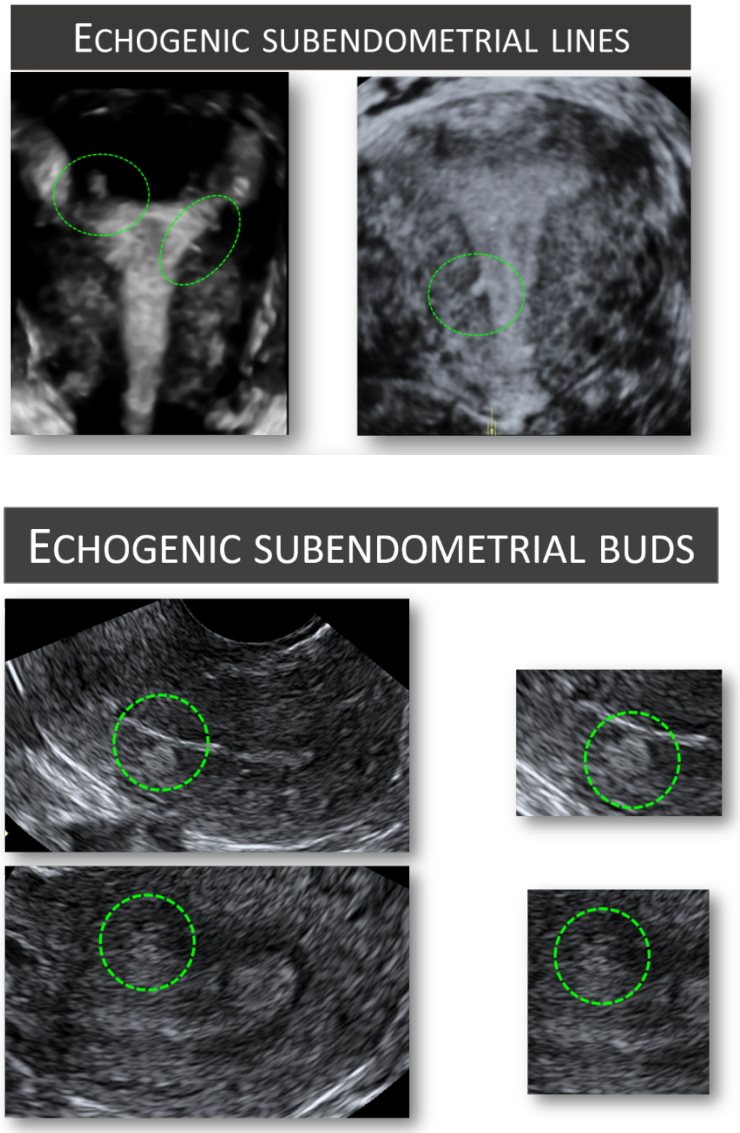

Figure 15: Normal vascular pattern of the myometrium

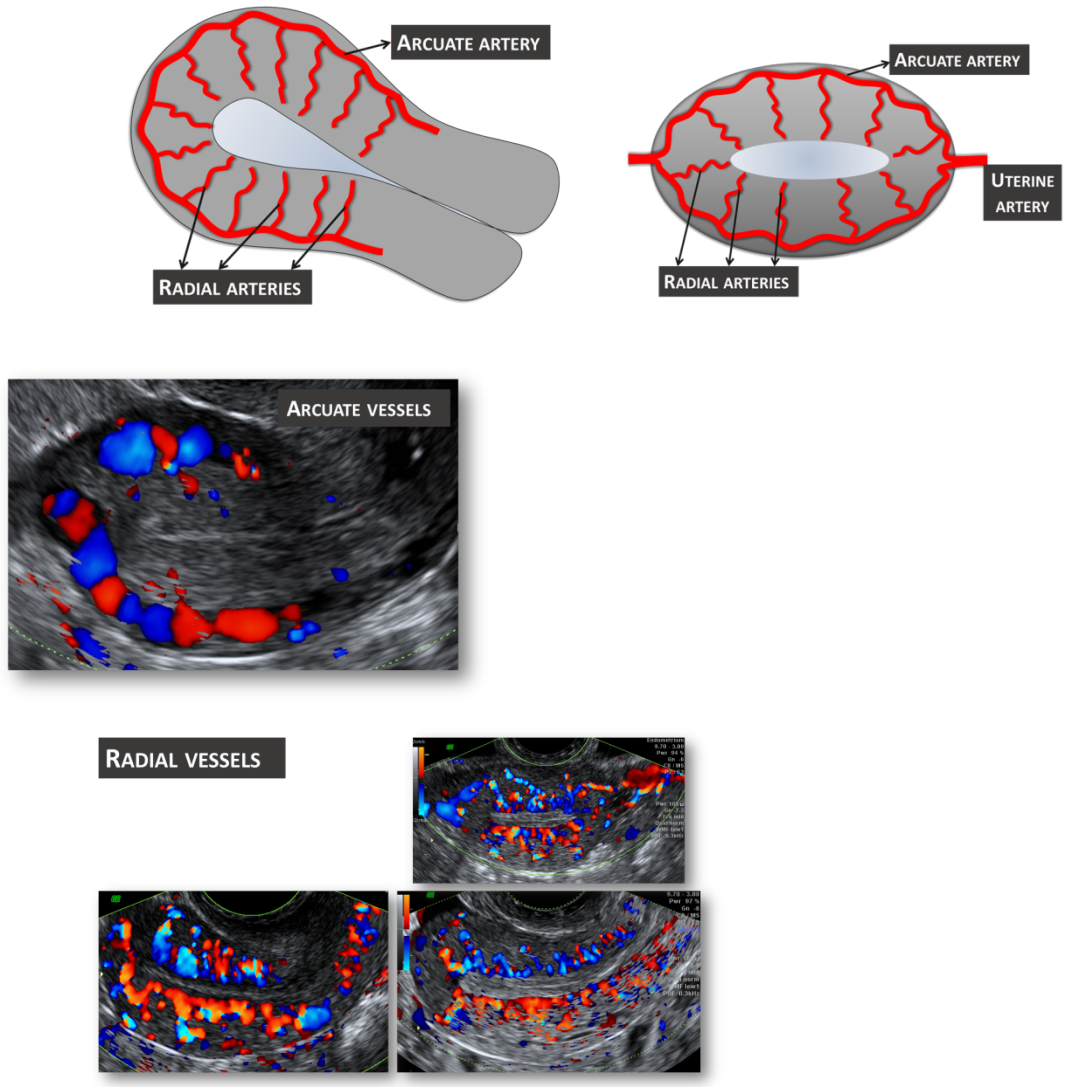

Figure 15: *Schematic drawings (upper row) and ultrasound images (lower rows) illustrating the normal vascular pattern of the myometrium. The arcuate vessels of the uterus are visible at the periphery of the myometrium, parallel to the uterine serosa. Perpendicular to the arcuate vessels, the radial arteries and veins flowing throughout the myometrium are usually detectable.*

Figure 16: Vascular pattern within the myometrium

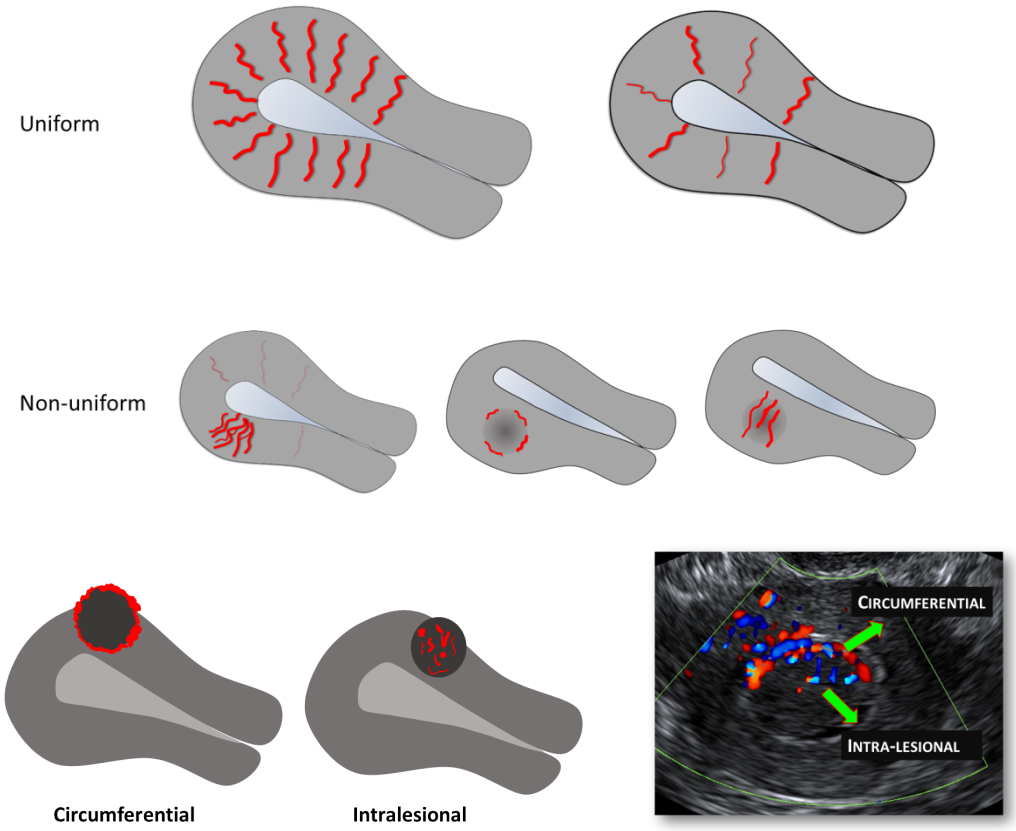

Figure 16. Schematic and ultrasound images illustrating the vascular pattern within the myometrium and in myometrial lesions. The vascular pattern of the myometrium may be uniform (upper row) or non-uniform (middle row). The vascular pattern of a myometrial lesion may be circumferential, intra-lesional or both circumferential and intra-lesional (lower row).

Figure 17: Translesional vascularity

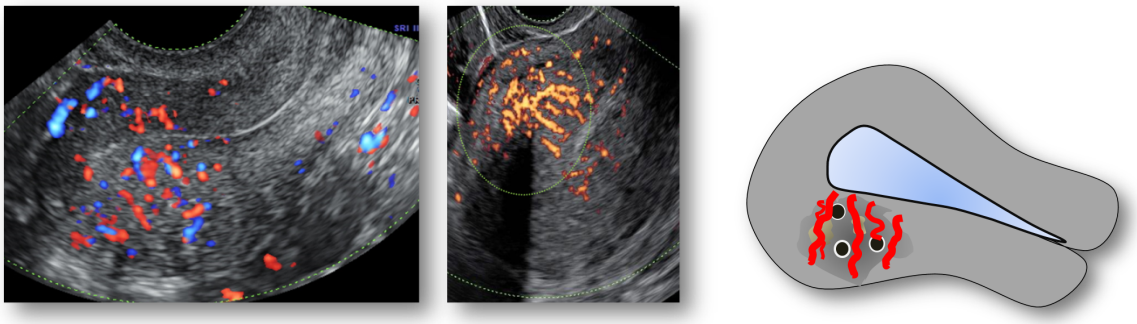

Figure 17*. Ultrasound images and a schematic drawing illustrating translesional vascularity which is defined as vessels perpendicular to the endometrium crossing the lesion.*

Figure 18: Color score of circumferential and intra-lesional vascularity.

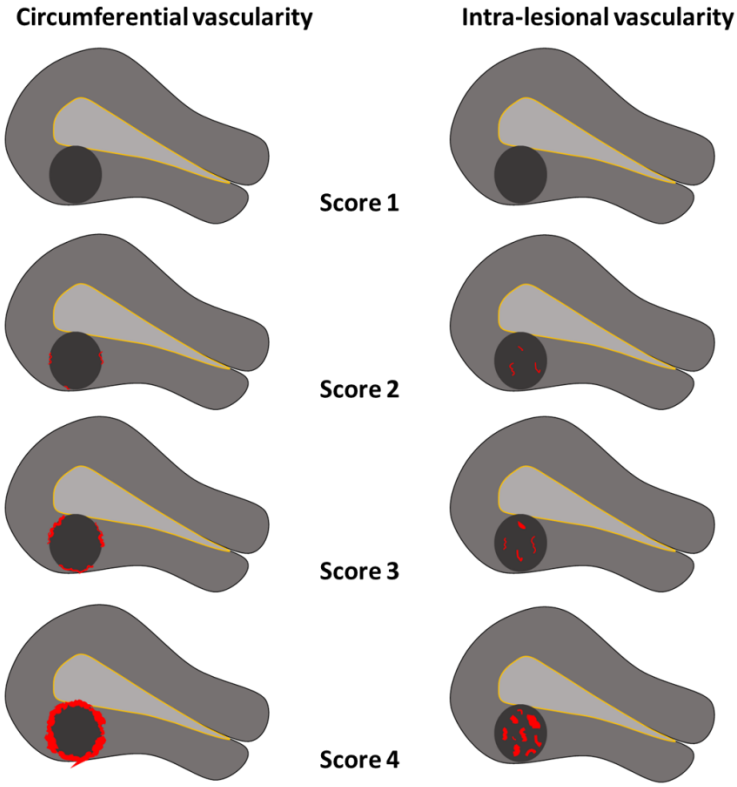

Figure 18. *Schematic images illustrating the color score (amount of color Doppler signals) in the circumference of and inside myometrial lesions. The amount of color is estimated subjectively. The color score is based on the subjective evaluation of both the percentage of the lesion being vascularized and the color hue. A color score of 1 represents no color, 2 minimal amount of color, 3 moderate and 4 abundant amount of color.*

Figure 19: Vascularization of a myometrial lesion: vessel number, size, branching and direction (for research purposes)

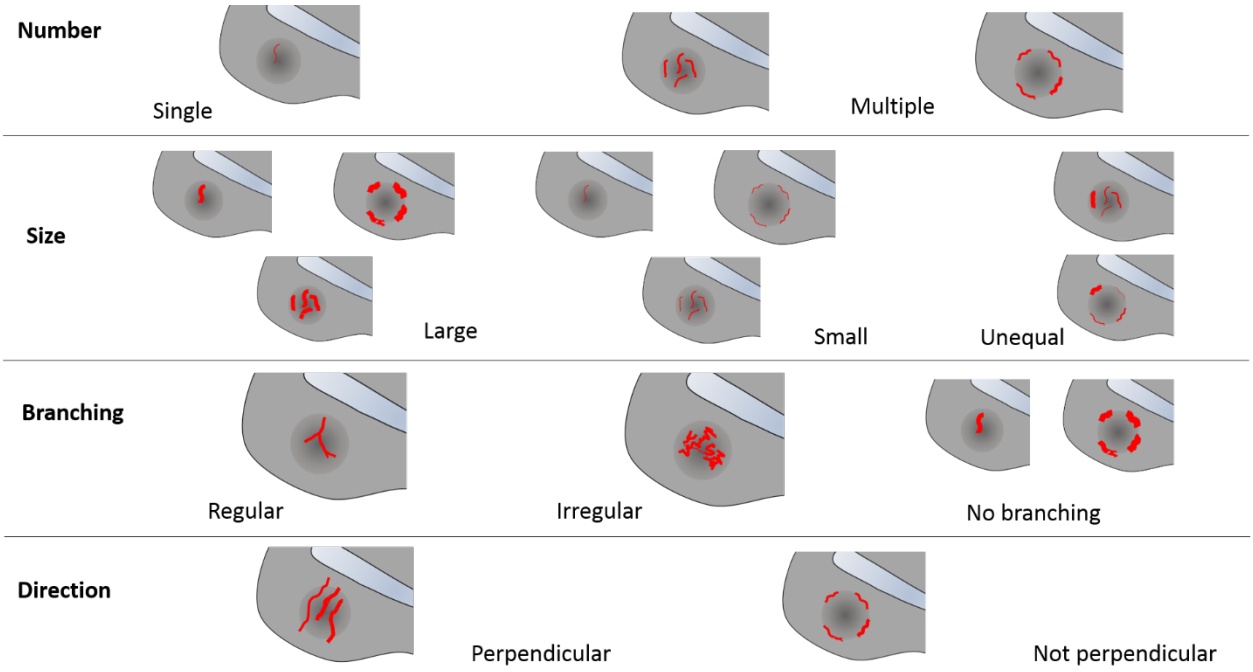

Figure 19. *Schematic drawings illustrating how to describe the vascularization of a myometrial lesion in clinical research, in terms of vessel number, vessel size (depending on the research protocol the vessel diameter may be measured), vessel branching and vessel direction. Circumferential vessels are the vessels surrounding a lesion.*

Figure 20: Schematic drawings illustrating the ultrasound features currently considered to be typical of adenomyosis.

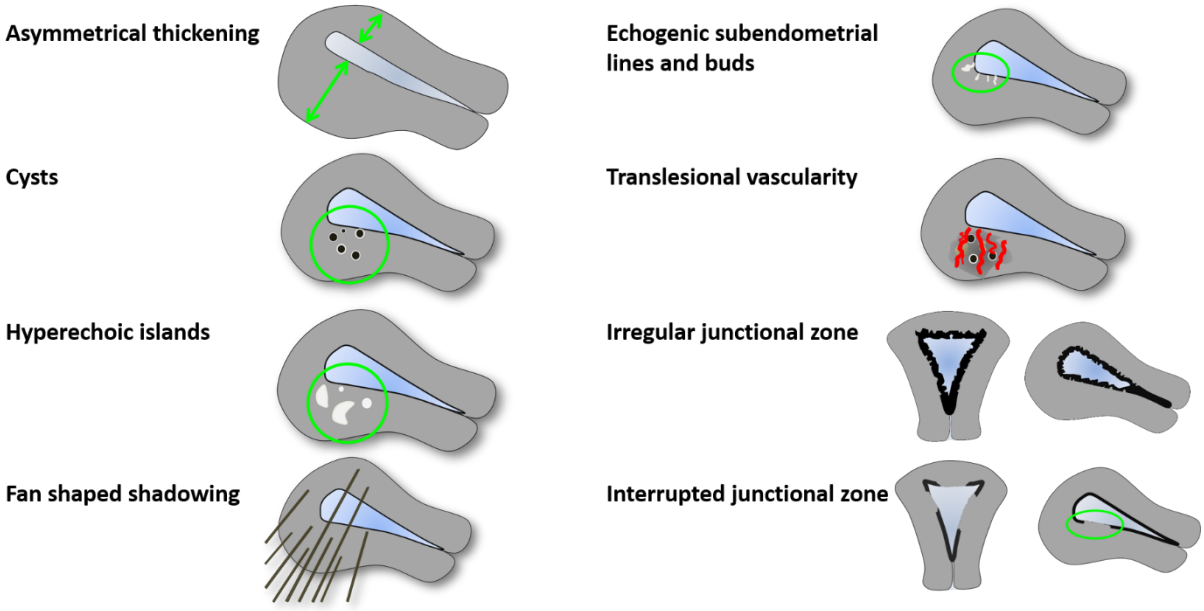

Figure 21: Schematic drawings illustrating the ultrasound features currently considered to be typical of uterine fibroids.

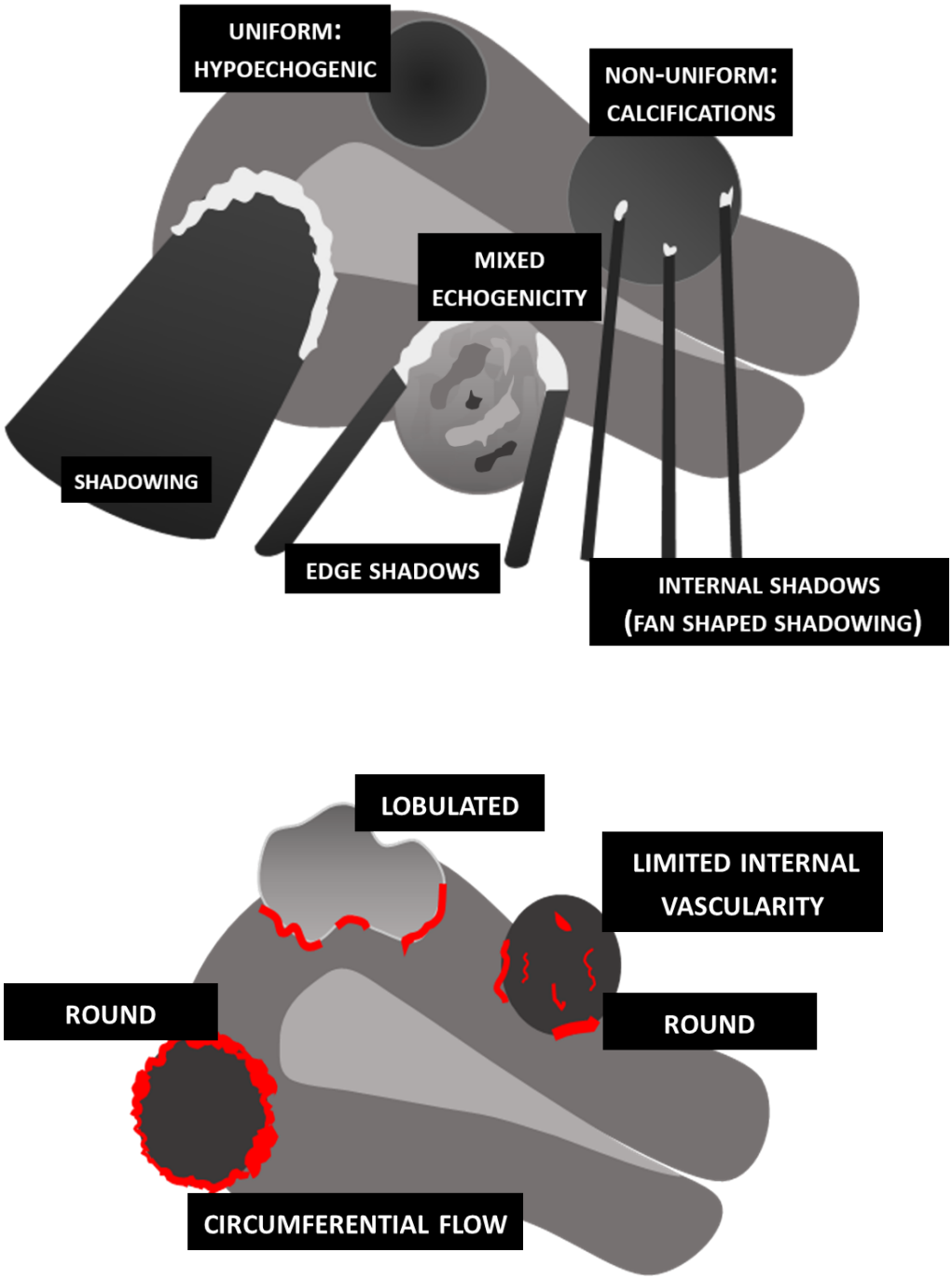

Figure 22: Ultrasound images showing fibroids with atypical sonographic features. These fibroid have a non-uniform echogenicity, intralesional anechoic cysts and some have areas with hyperechogenicity. There is an irregular outline of the FIGO type1 fibroid (lower right).

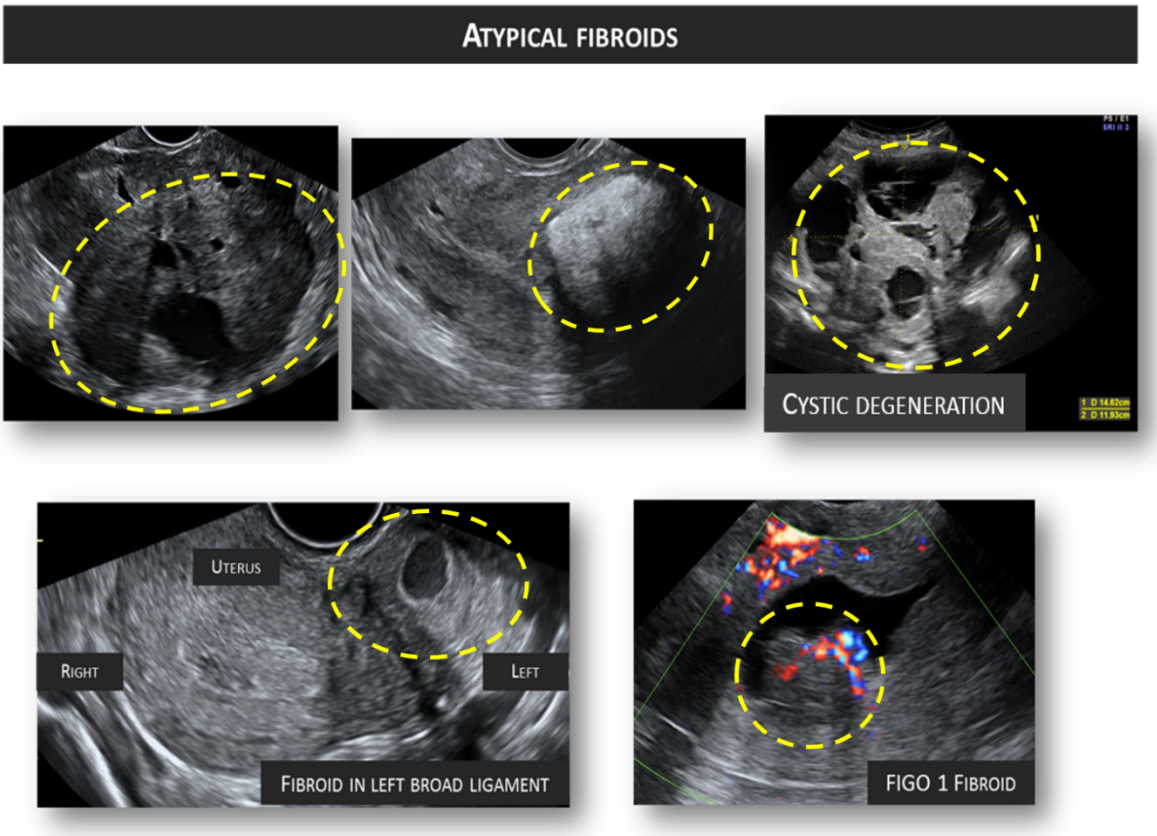

Figure 23: Gray scale and color Doppler images of a sarcoma in the anterior wall of the uterus. The uterine corpus (yellow arrows) is located posteriorly and contains clear fluid (green arrow).